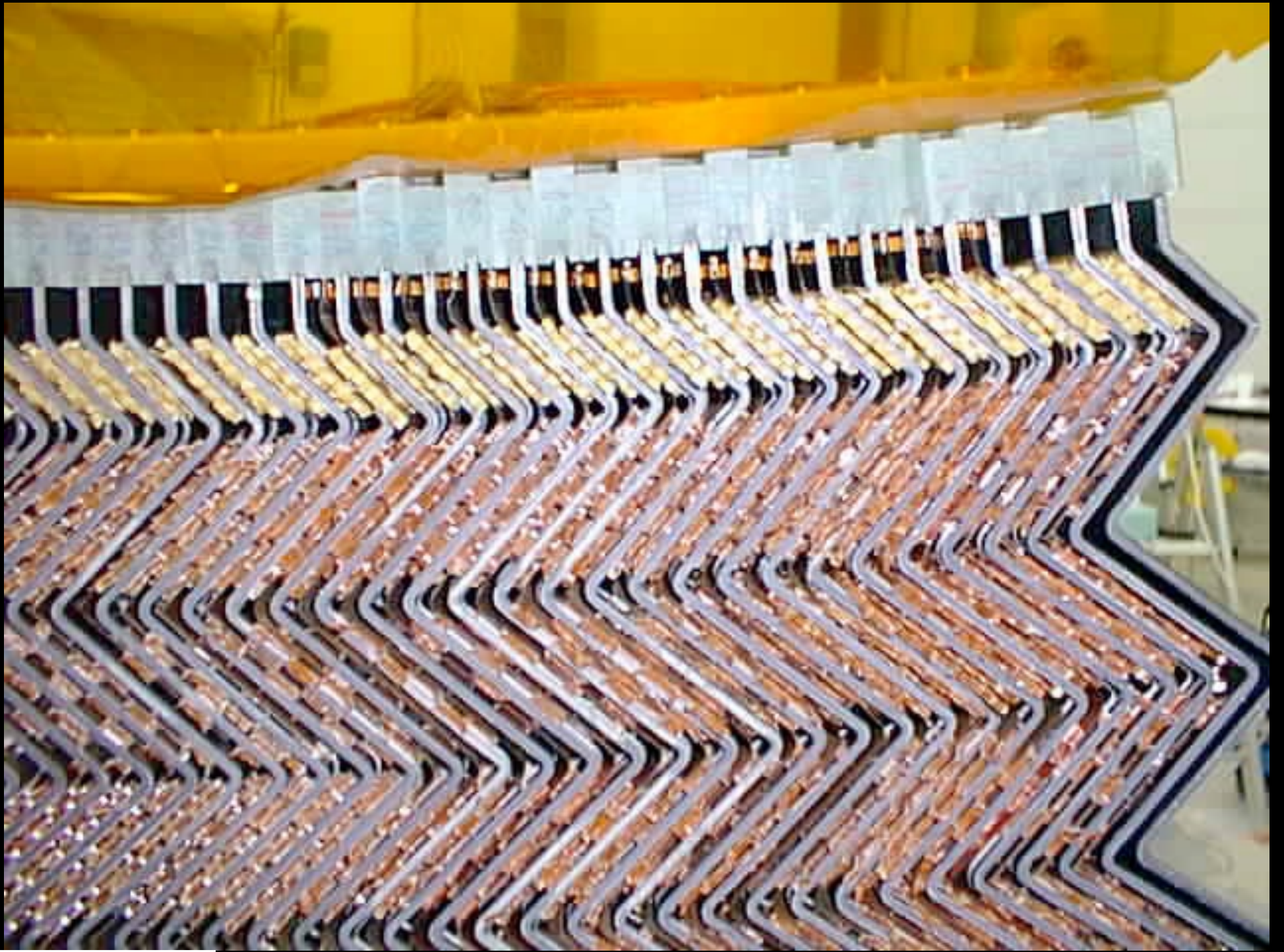


INSTRUMENTATION & DETECTORS for HIGH ENERGY PHYSICS V

isabelle.wingerter@lapp.in2p3.fr
Office: 40-4-D32 - tel: 16 4889



2000 - 2003



2004



TODAY

CALORIMETRY-2

&

A FEW EXAMPLES

HADRONIC SHOWERS

Hadronic cascades develop in an analogous way to e.m. showers

Strong interaction controls overall development

High energy hadron interacts with material, leading to multi-particle production of more hadrons

These in turn interact with further nuclei

Nuclear breakup and spallation neutrons

Multiplication continues down to the pion production threshold

$$E \sim 2m_{\pi} = 0.28 \text{ GeV}/c^2$$

Neutral pions result in an electromagnetic component (immediate decay: $\pi^0 \rightarrow \gamma\gamma$)
(also: $\eta \rightarrow \gamma\gamma$)

Energy deposited by:

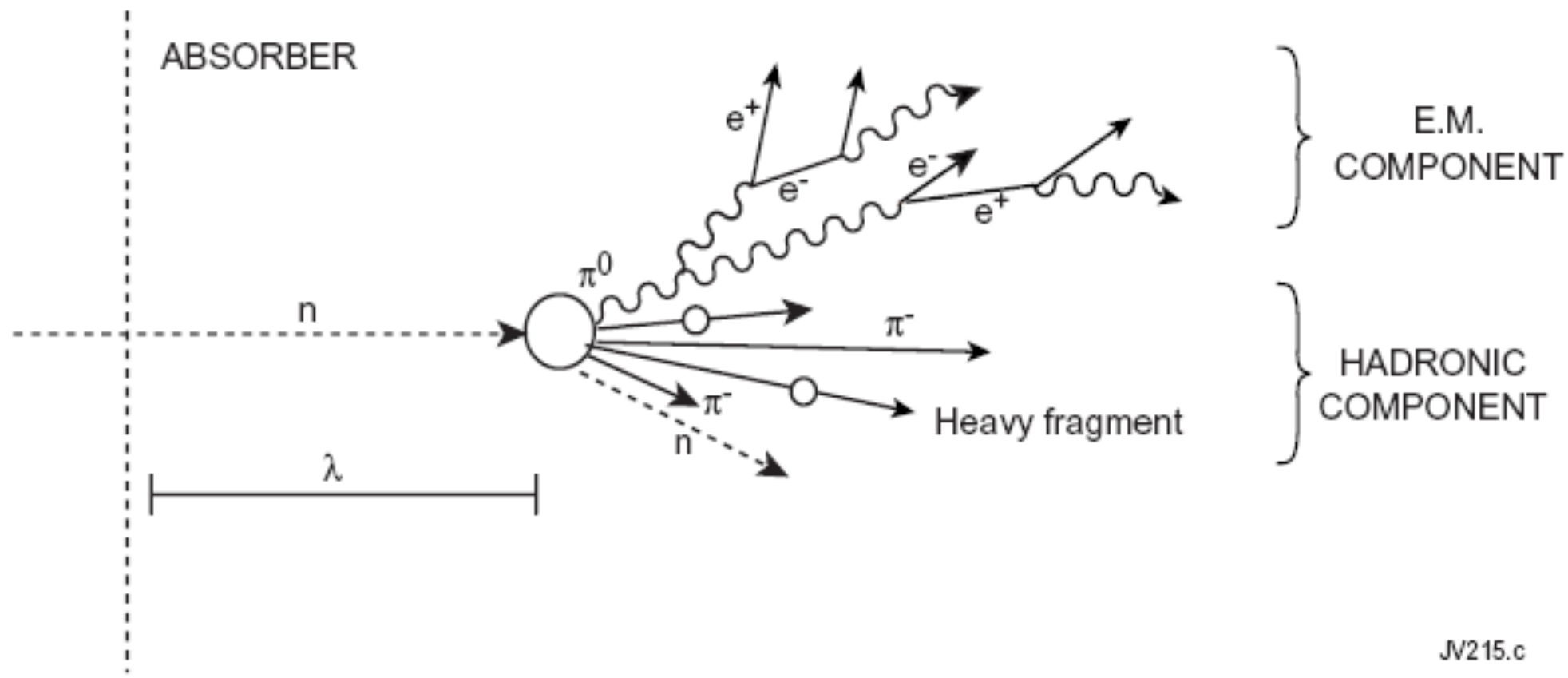
Electromagnetic component (i.e. as for e.m. showers)

Charged pions or protons

Low energy neutrons

Energy lost in breaking nuclei (nuclear binding energy)

HADRONIC CASCADE



JV215.c

As compared to electromagnetic showers, hadron showers are:

- Larger/more penetrating
- Subject to larger fluctuations – more erratic and varied

HADRONIC SHOWERS: WHERE DOES THE ENERGY GO ?

	<i>Lead</i>	<i>Iron</i>
Ionization by pions	19%	21%
Ionization by protons	37%	53%
<i>Total ionization</i>	56%	74%
Nuclear binding energy loss	32%	16%
Target recoil	2%	5%
<i>Total invisible energy</i>	34%	21%
Kinetic energy evaporation neutrons	10%	5%
Number of charged pions	0.77	1.4
Number of protons	3.5	8
Number of cascade neutrons	5.4	5
Number of evaporation neutrons	31.5	5
Total number of neutrons	36.9	10
Neutrons/protons	10.5/1	1.3/1

HADRONIC INTERACTION

Simple model of interaction on a disk of radius R: $\sigma_{\text{int}} = \pi R^2 \propto A^{2/3}$

$$\sigma_{\text{inel}} \approx \sigma_0 A^{0.7}, \quad \sigma_0 = 35 \text{ mb}$$

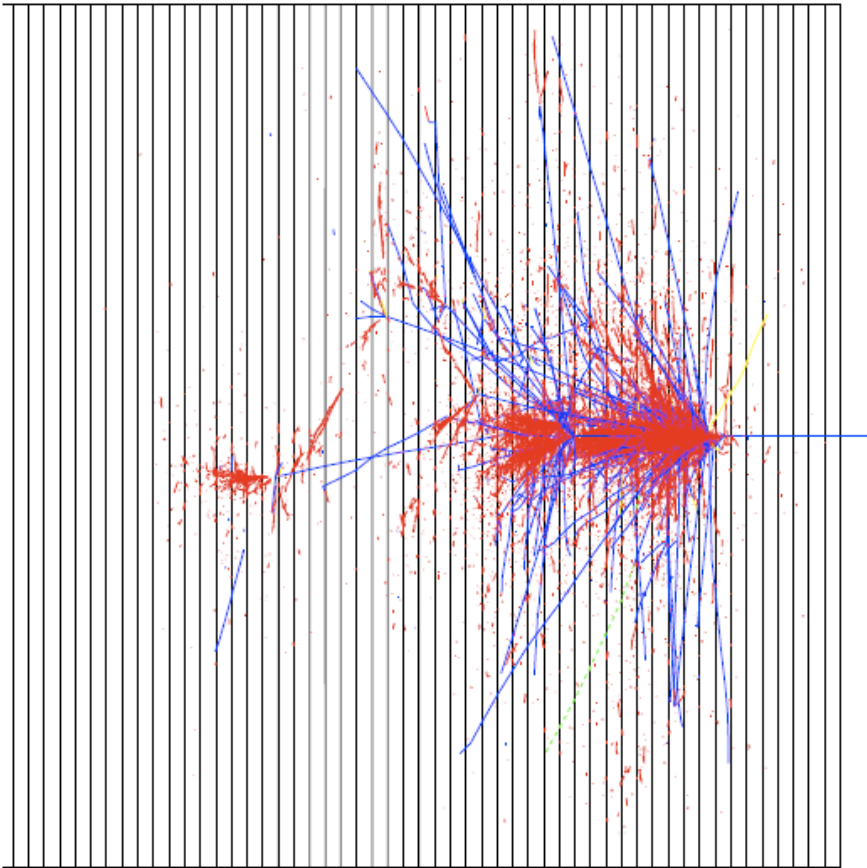
Nuclear interaction length: mean free path before inelastic interaction

$$\lambda_{\text{int}} \approx \frac{A}{N_A \sigma_{\text{int}}} \approx 35 A^{1/3} \text{ g cm}^{-2}$$

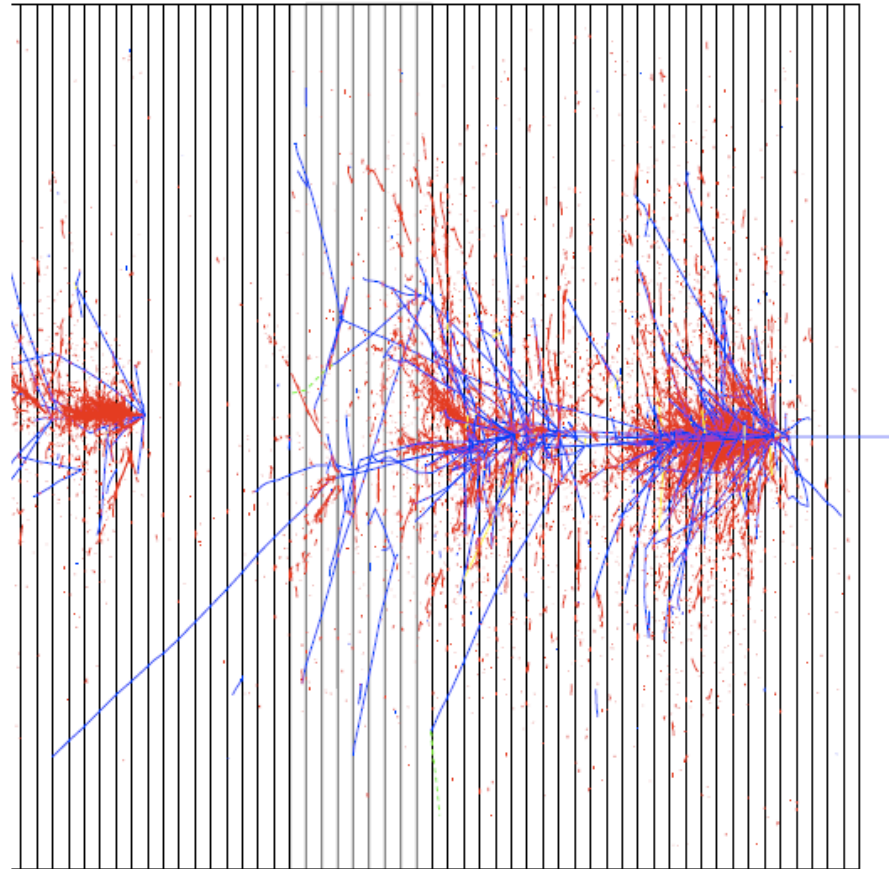
	Z	ρ (g.cm ⁻³)	E_c (MeV)	X_0 (cm)	λ_{int} (cm)
Air				30 420	~70 000
Water				36	84
PbWO ₄		8.28		0.89	22.4
C	6	2.3	103	18.8	38.1
Al	13	2.7	47	8.9	39.4
L Ar	18	1.4		14	84
Fe	26	7.9	24	1.76	16.8
Cu	29	9	20	1.43	15.1
W	74	19.3	8.1	0.35	9.6
Pb	82	11.3	6.9	0.56	17.1
U	92	19	6.2	0.32	10.5

HADRONIC SHOWERS

1. Individual hadron showers are quite dissimilar

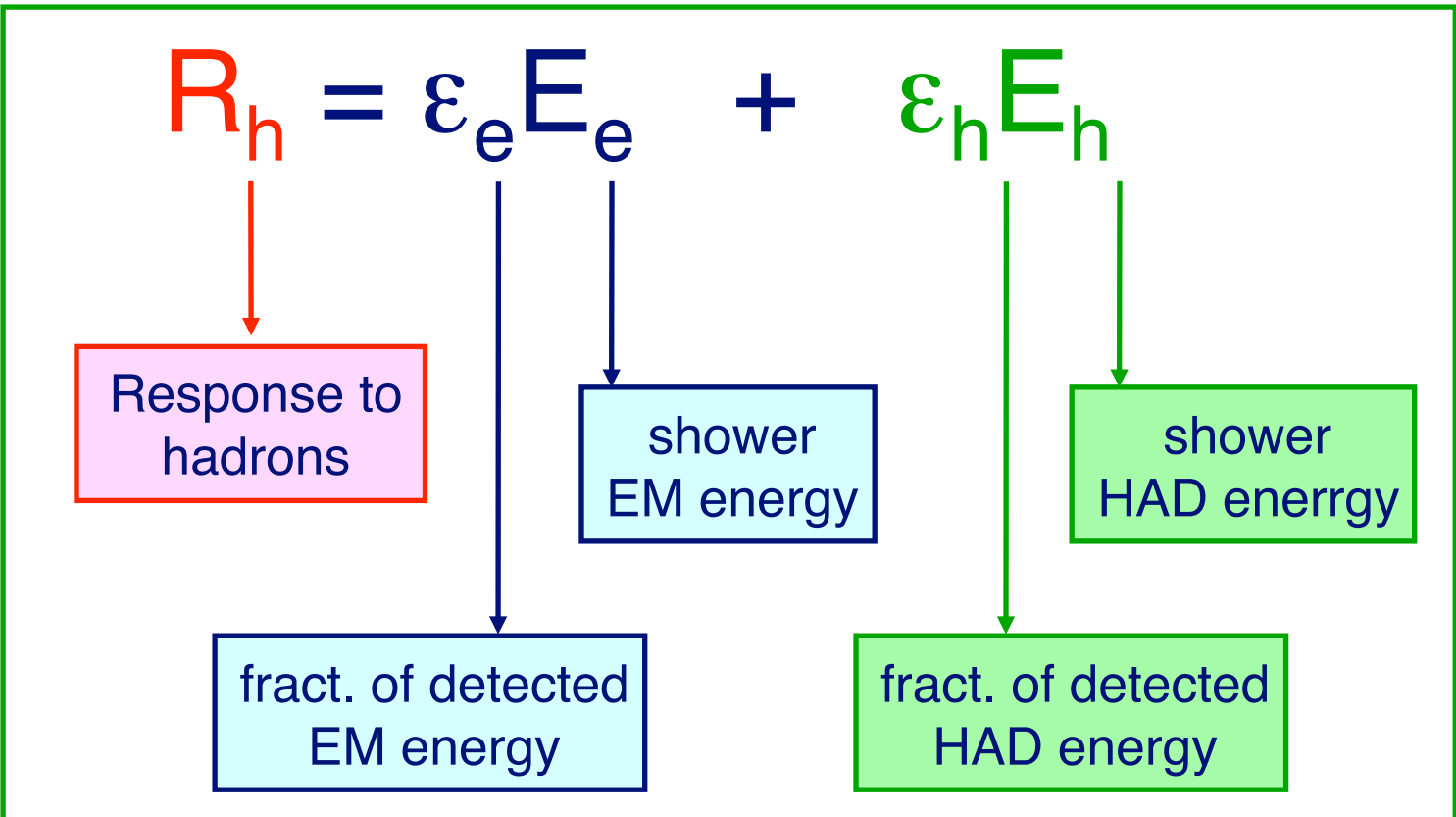


2.



red - e.m. component
blue - charged hadrons

HADRONIC SHOWERS and NON-COMPENSATION



$$\frac{e}{h} = \frac{\epsilon_e}{\epsilon_h}$$

≈ 1 : compensating calorimeter

> 1 : non compensating calorimeter

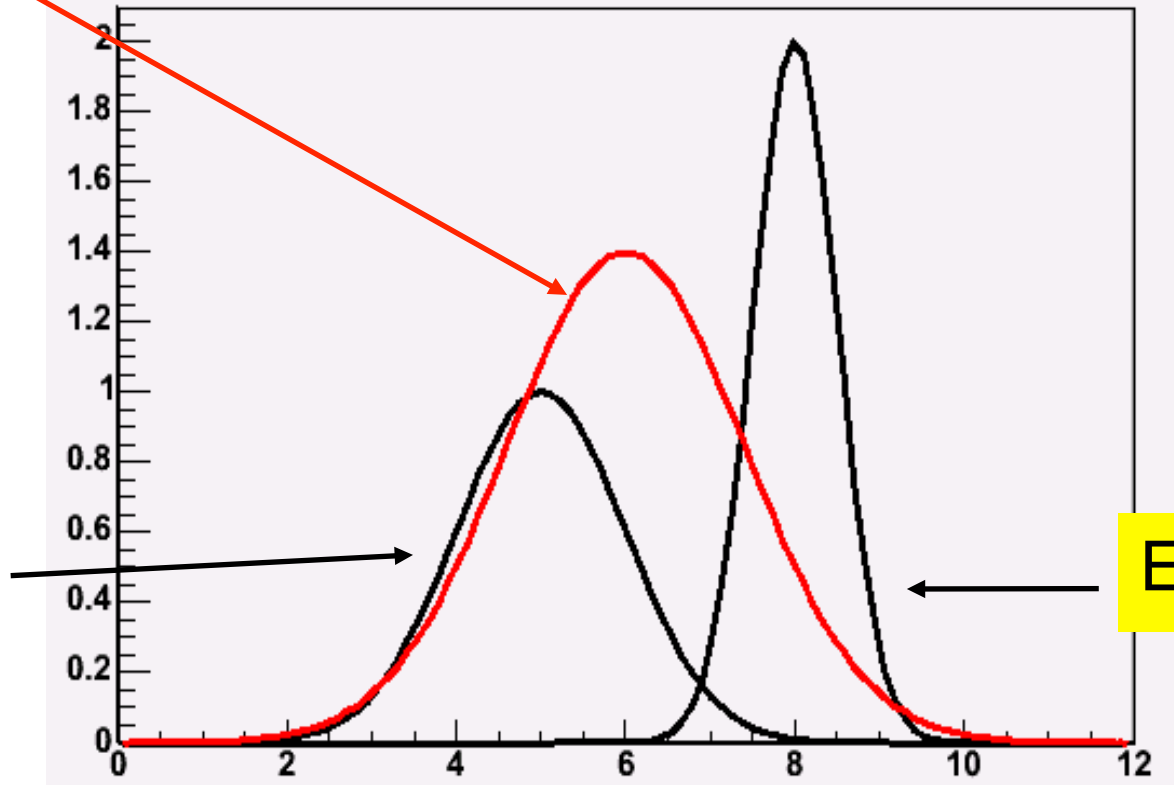
HADRONIC SHOWERS and NON-COMPENSATION

$$R_h = \epsilon_e E_e + \epsilon_h E_h$$

$$\epsilon_e > \epsilon_h$$

$$E_e \ll E_h$$

$$E_e \gg E_h$$



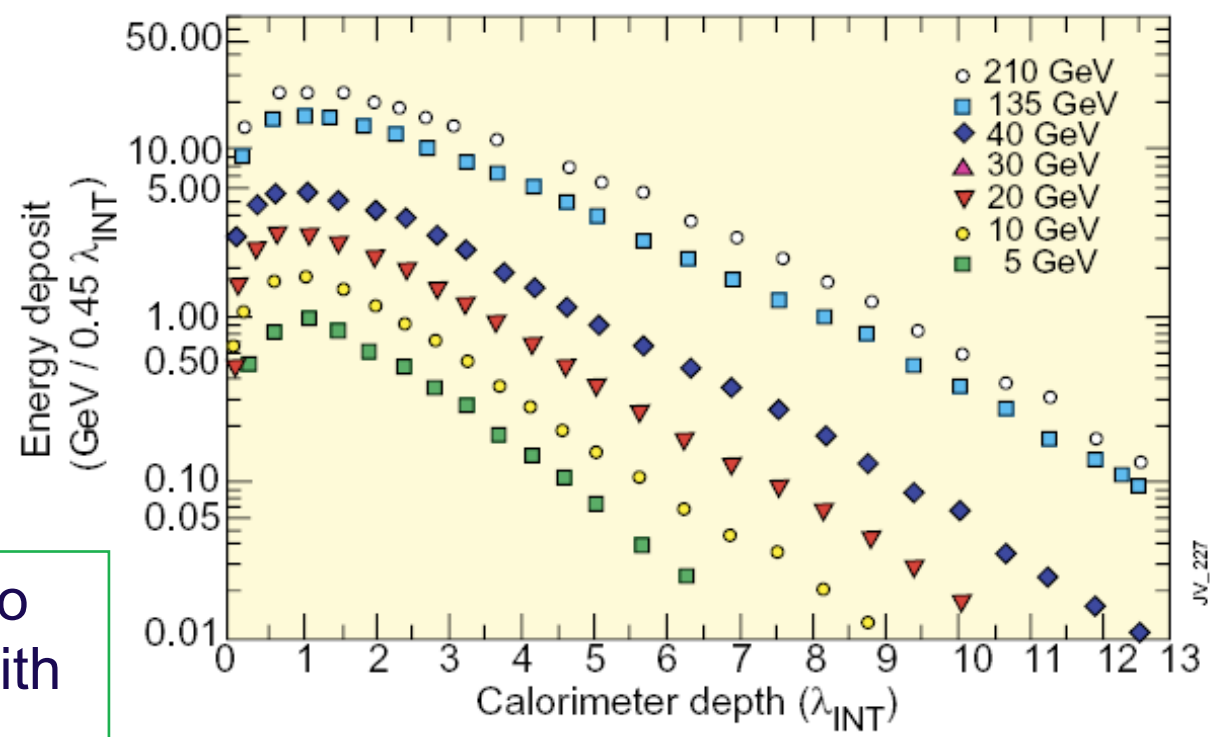
HADRONIC SHOWER LONGITUDINAL DEVELOPMENT

Longitudinal profile

Initial peak from π^0 s produced in the first interaction length

Gradual falloff characterised by the nuclear interaction length, λ_{int}

WA78 : 5.4 λ of 10mm U / 5mm Scint + 8 λ of 25mm Fe / 5mm Scint



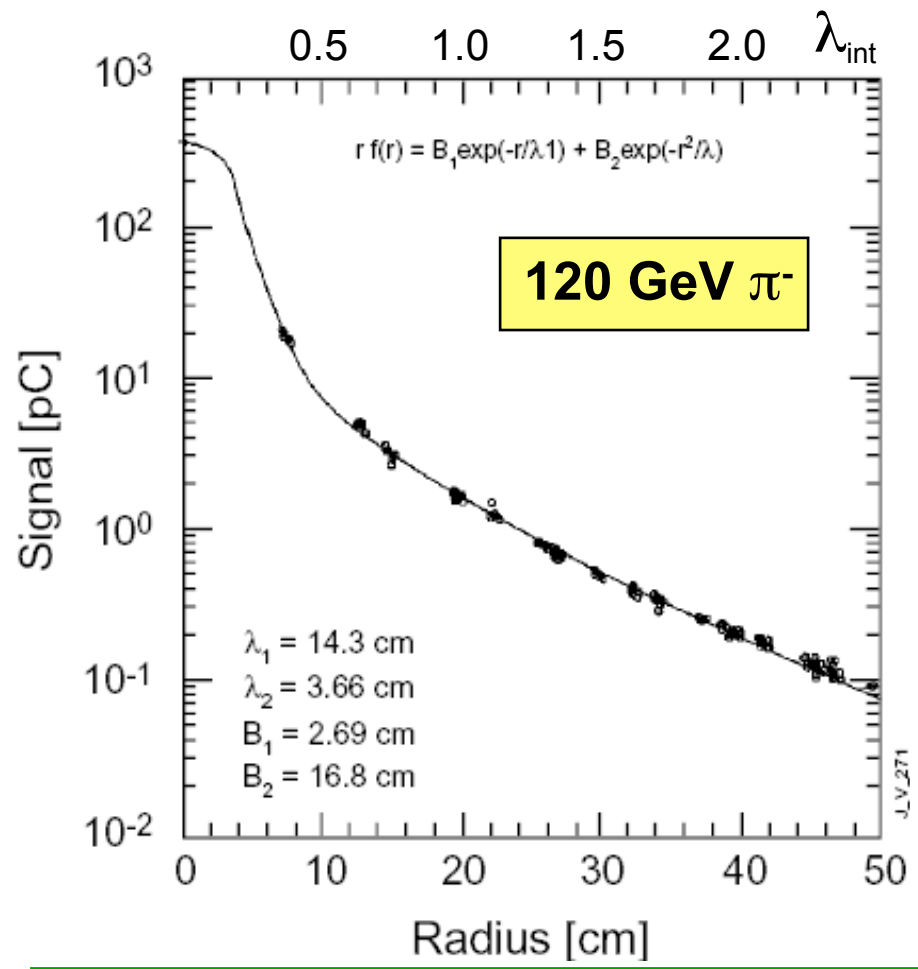
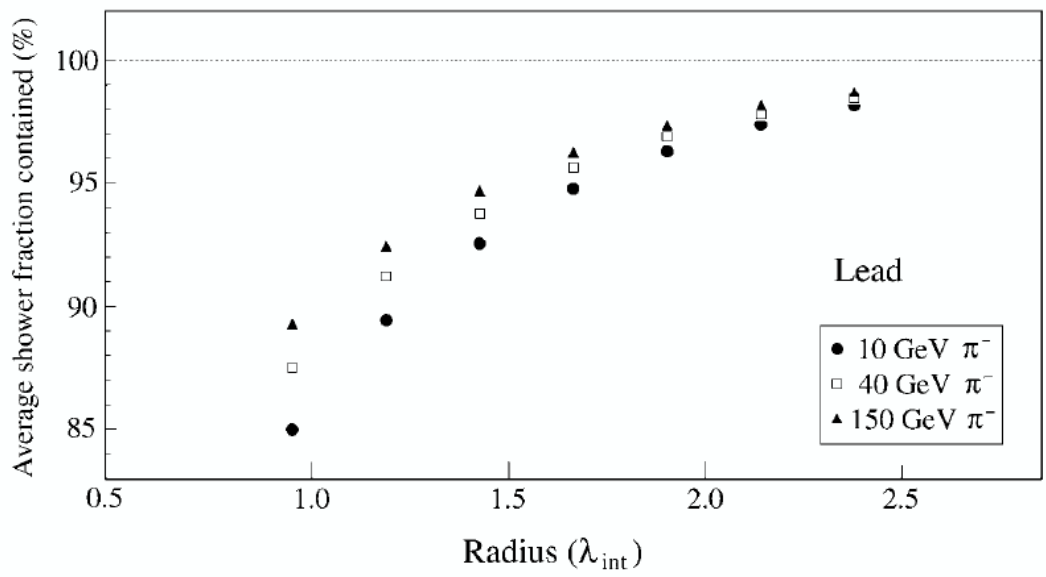
As with e.m. showers: depth to contain a shower increases with $\log(E)$

HADRONIC SHOWERS TRANSVERSE PROFILE

Mean transverse momentum from interactions, $\langle p_T \rangle \sim 300$ MeV, is about the same magnitude as the energy lost traversing 1λ for many materials

So radial extent of the cascade is well characterized by λ

The π^0 component of the cascade results in an electromagnetic core



Lateral containment increases with energy

JETS at HIGH ENERGY COLLIDERS

At Hadronic Colliders, quarks & gluons produced, evolves (parton shower, hadronisation) to become jets

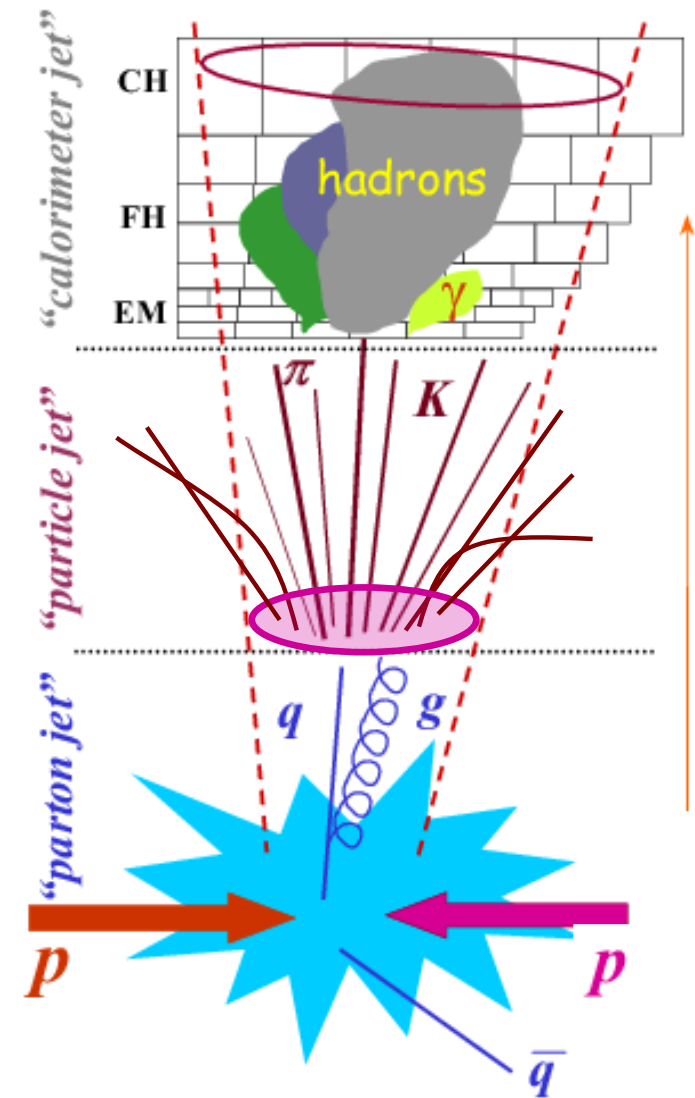
In a cone around the initial parton: high density of hadrons

LHC calorimeters cannot separate all the incoming hadrons

Use dedicated calibration schemes (based on simulation in ATLAS)

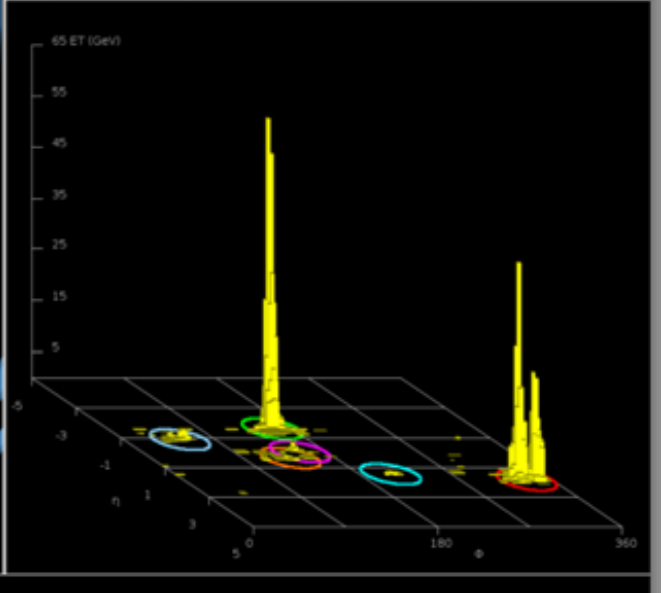
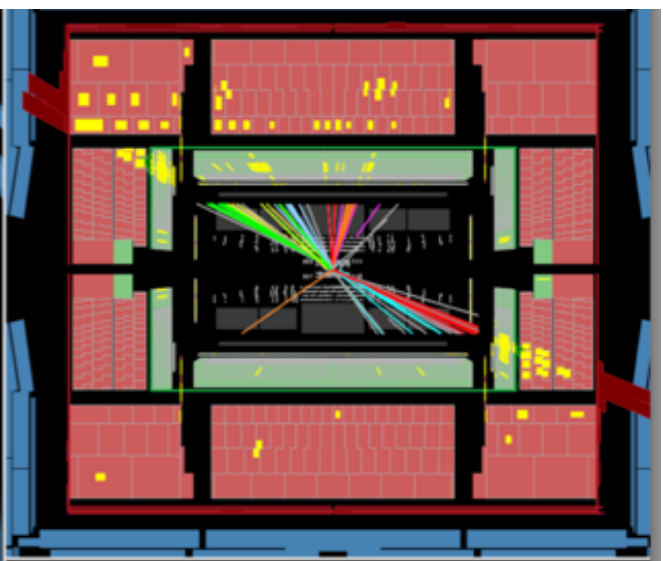
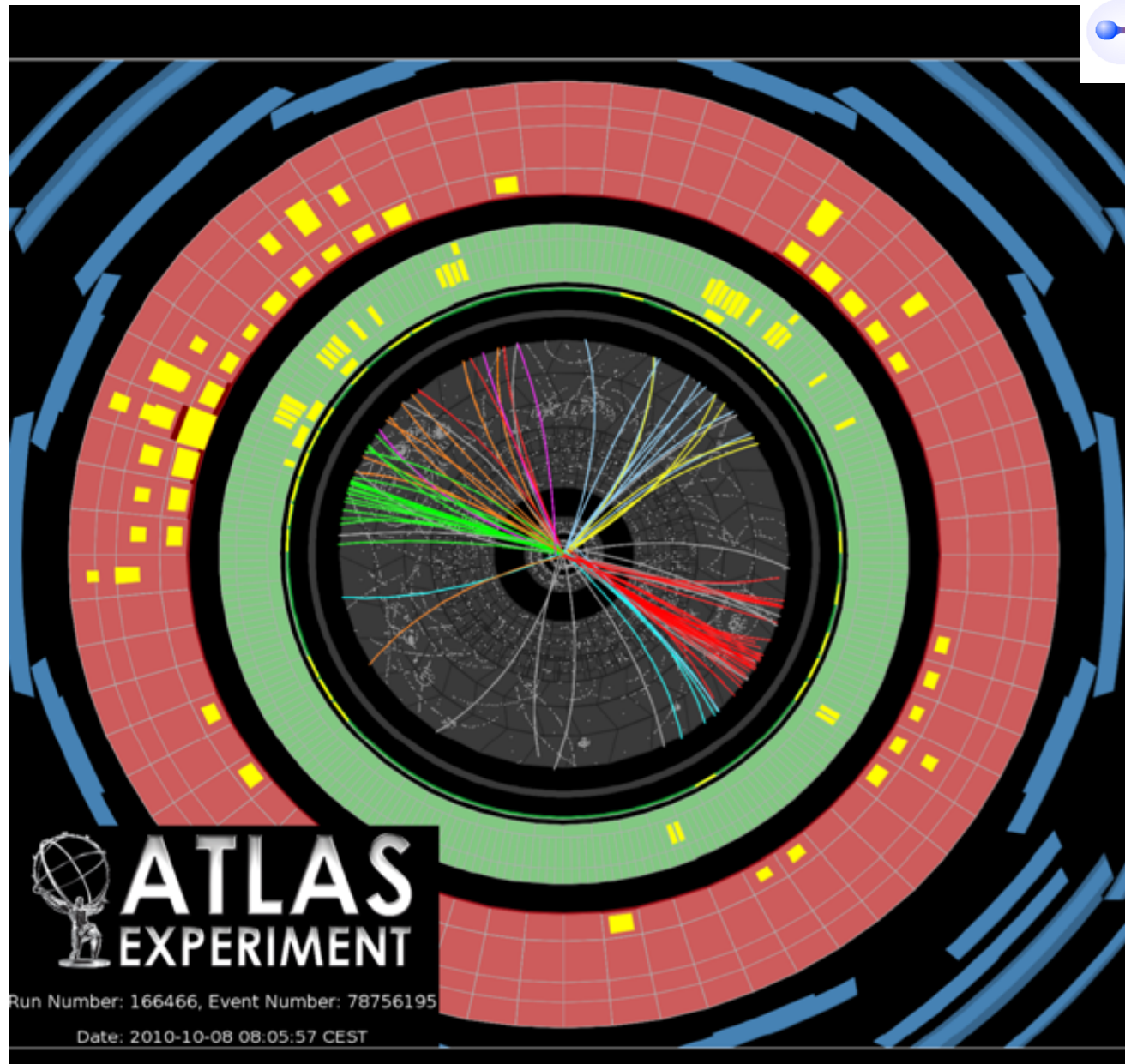
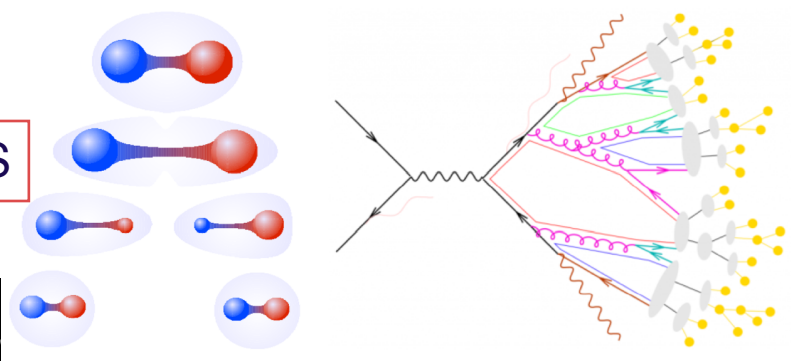
Use tracking system to identify charged hadrons (Particle Flow in CMS)

In the future, very highly segmented calorimeters



JETS

NEED a REFINED CALIBRATION PROCEDURE FOR JETS

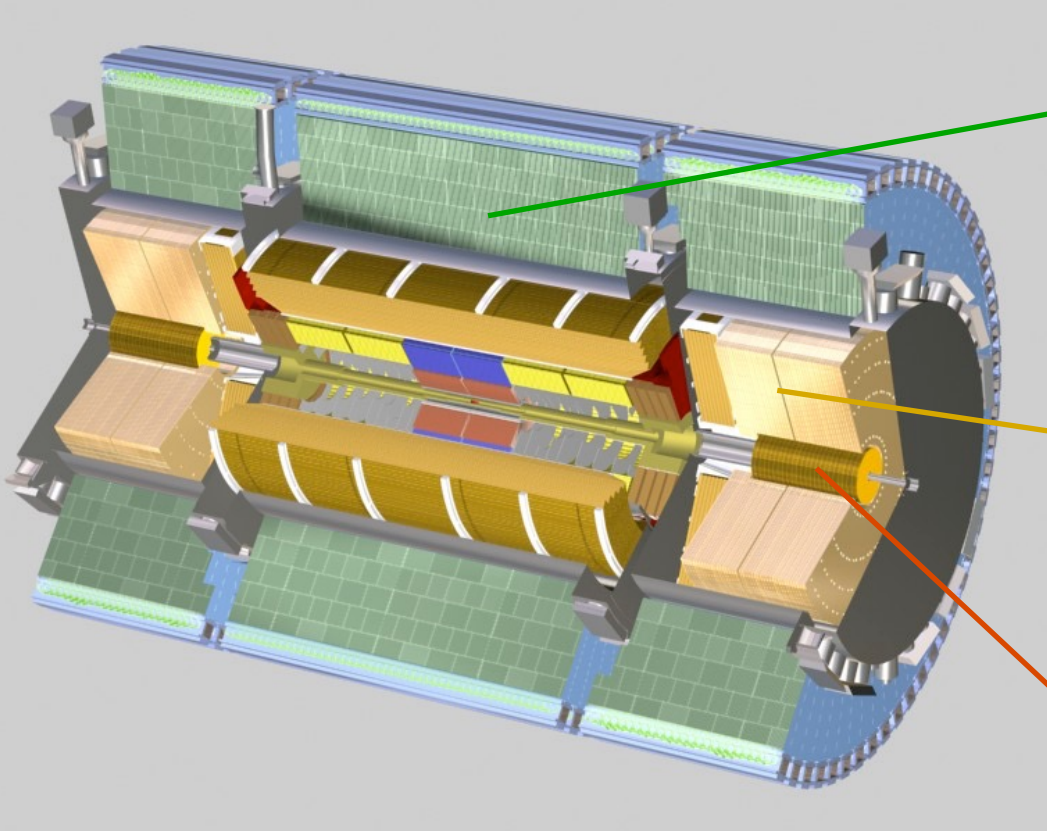


ATLAS
EXPERIMENT

Run Number: 166466, Event Number: 78756195

Date: 2010-10-08 08:05:57 CEST

ATLAS HADRON CALORIMETER



Tiles Calorimeter $|\eta| < 1.7$
 Fe / Scintillator
 3 layers in depth

LAr/Cu $1.7 < |\eta| < 3.2$
 4 layers in depth

Forward: 1 layer EM, 2 HAD
 LAr/Cu or W $3.2 < |\eta| < 4.9$

Total thickness: $\sim 8 - 10 \lambda$
 Use of different technics: cope with radiations in forward region

Scintillator tile calorimeter

	Barrel	Extended barrel
$ \eta $ coverage	$ \eta < 1.0$	$0.8 < \eta < 1.7$
Number of layers	3	3
Granularity $\Delta\eta \times \Delta\phi$	0.1×0.1	0.1×0.1
Last layer	0.2×0.1	0.2×0.1
Readout channels	5760	4092 (both sides)

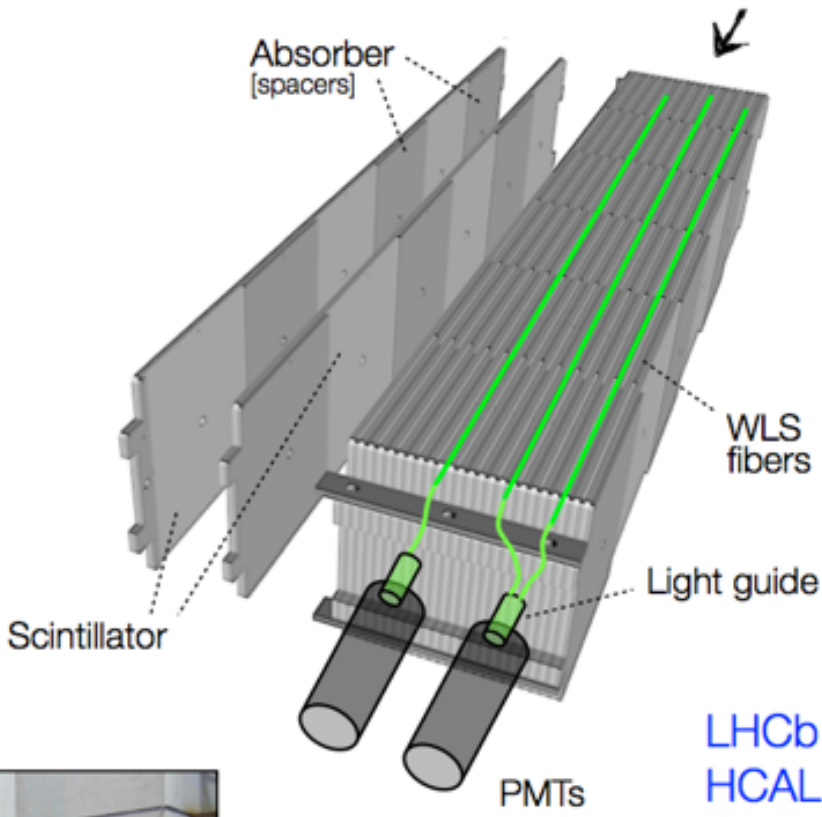
HADRONIC CALORIMETER

Most common realization: **Sampling Calorimeter**

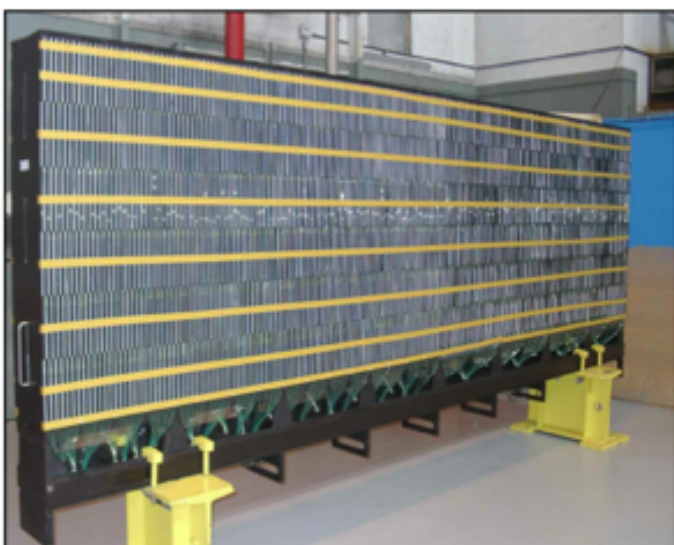
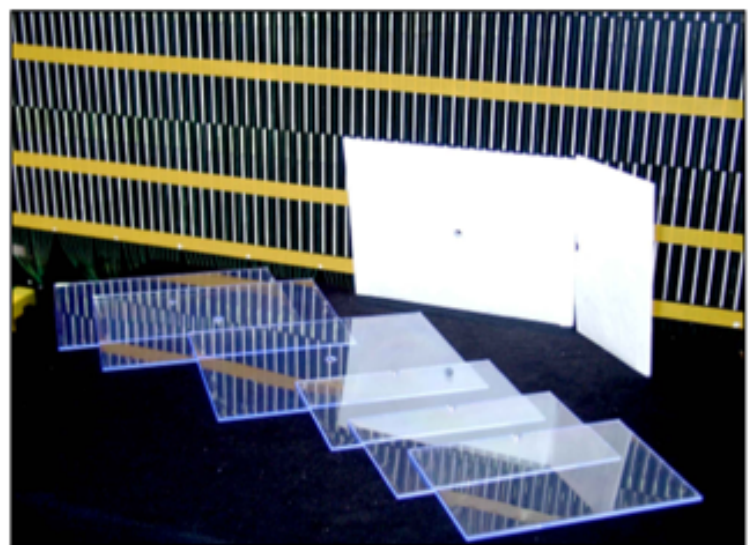
Utilization of homogenous calorimeters unnecessary (and thus too expensive) due to fluctuations of invisible shower components ...

Typical absorbers : Fe, Pb, U ...
Sampling elements : Scintillators, LAr, MWPCs ...

Typical setup:
Alternating layers of active and passive material
[also: 'spaghetti' or 'shashlik' calorimeter]



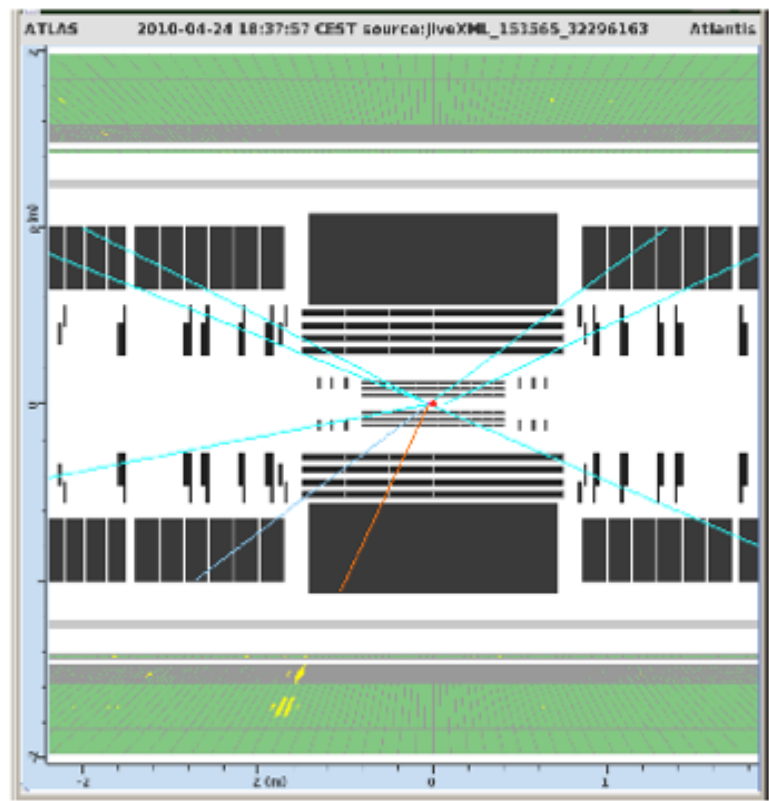
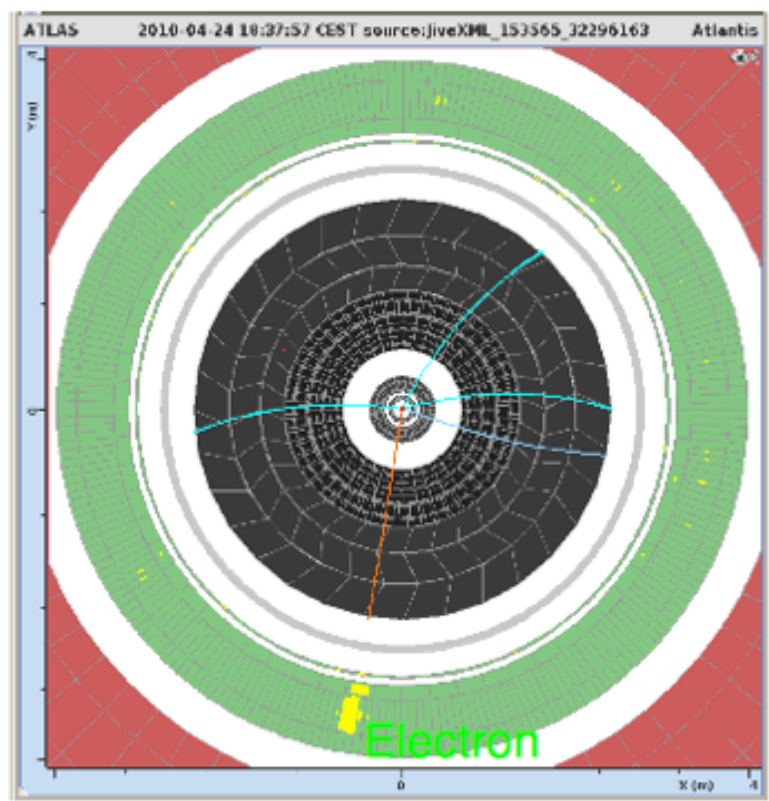
LHCb
HCAL



Example:
LHCb Hadron Calorimeter

MISSING TRANSVERSE ENERGY

Missing transverse energy : $W \rightarrow e \nu$ candidate



For a pp collision, for instance, and in the absence of escaping particles (neutrinos, neutralinos, DM,..) the transverse energy is ~balanced.

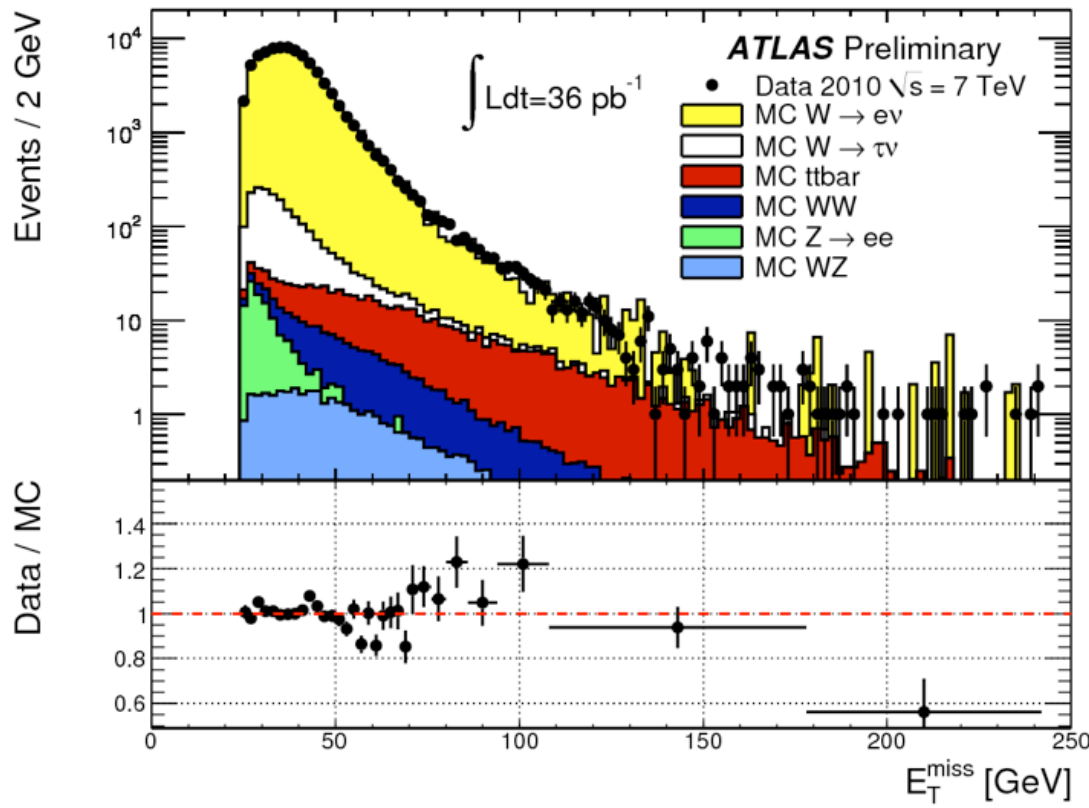
Missing transverse energy is interpreted as the presence of a neutrino.

$$\vec{E}_T^{miss} = - \sum_i^{cells} \vec{E}_T$$

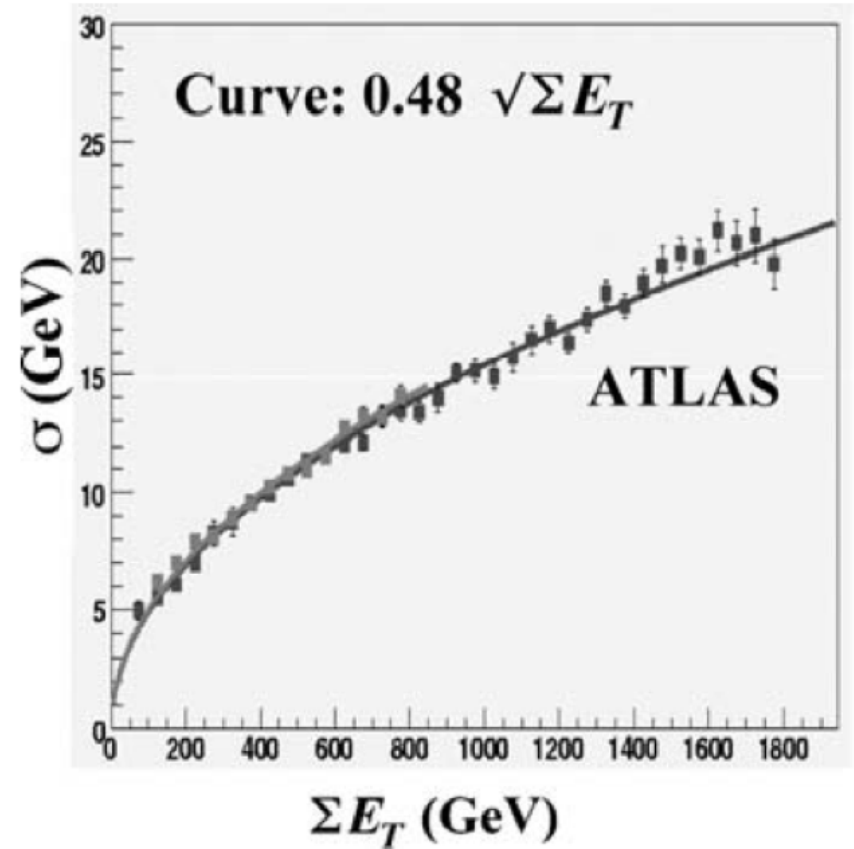
E_T^{miss} is the modulus of the vectorial sum of energy deposited in each calorimeter cell

MISSING TRANSVERSE ENERGY: CALIBRATION

Missing transverse energy in ATLAS for $W \rightarrow e\nu$ events



Missing transverse energy expected resolution in ATLAS



A FEW SUMMARY WORDS on CALORIMETERS

Calorimeters are attractive in our field for various reasons:

In contrast with magnet spectrometers, in which the momentum resolution deteriorates linearly with the particle momentum, on most cases the calorimeter energy resolution improves as $1/\text{Sqrt}(E)$, where E is the energy of the incident particle. Therefore calorimeters are very well suited for high-energy physics experiments.

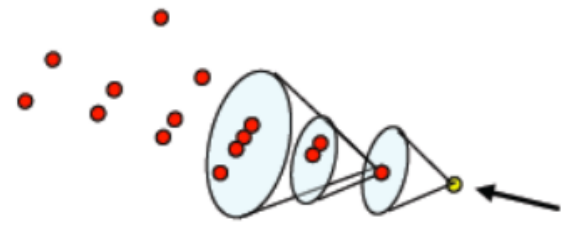
In contrast to magnet spectrometers, calorimeters are sensitive to all types of particles, charged and neutral. They can even provide indirect detection of neutrinos and their energy through a measurement of the event missing energy.

Calorimeters are commonly used for trigger purposes since they can provide fast signals that are easy to process and interpret.

They are space and therefore cost effective. Because the shower length increases only logarithmically with energy, the detector thickness needs to increase only logarithmically with the energy of the particles. In contrast for a fixed momentum resolution, the bending power BL^2 of a magnetic spectrometer must increase linearly with the particle momentum.

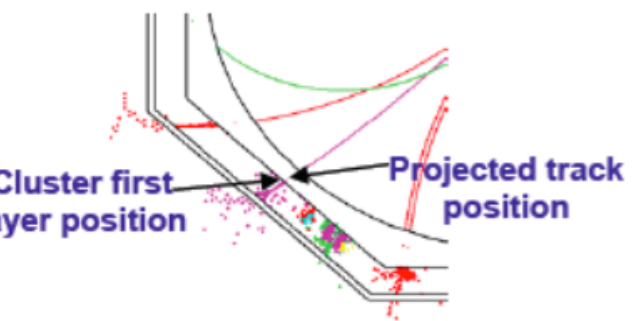
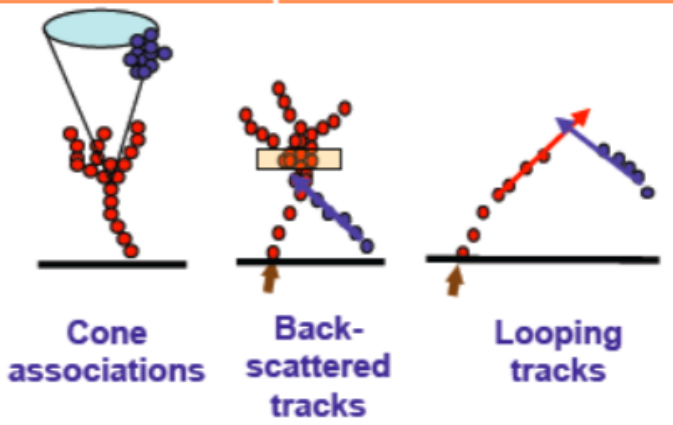
PARTICLE FLOW

Mark Thomson



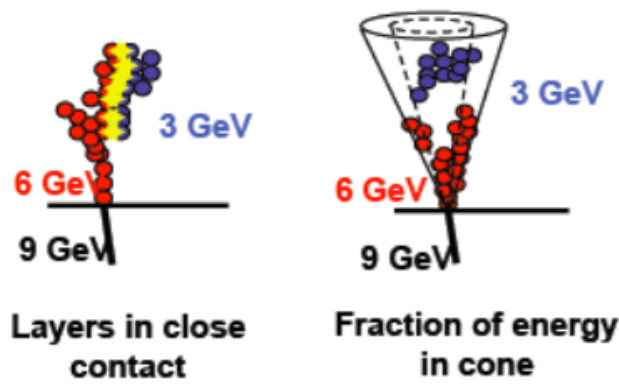
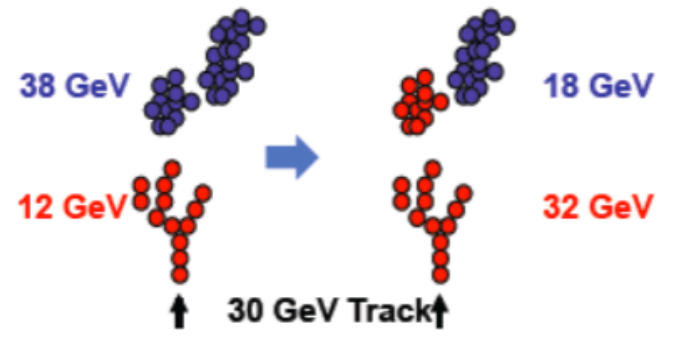
ConeClustering Algorithm

Topological Association Algorithms



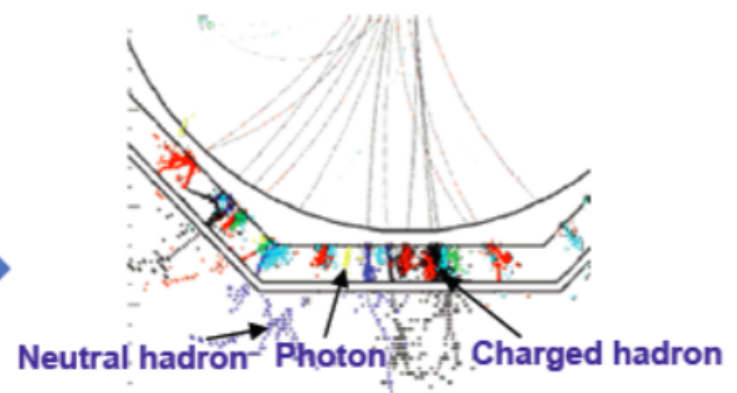
Track-Cluster Association Algorithms

Reclustering Algorithms



Fragment Removal Algorithms

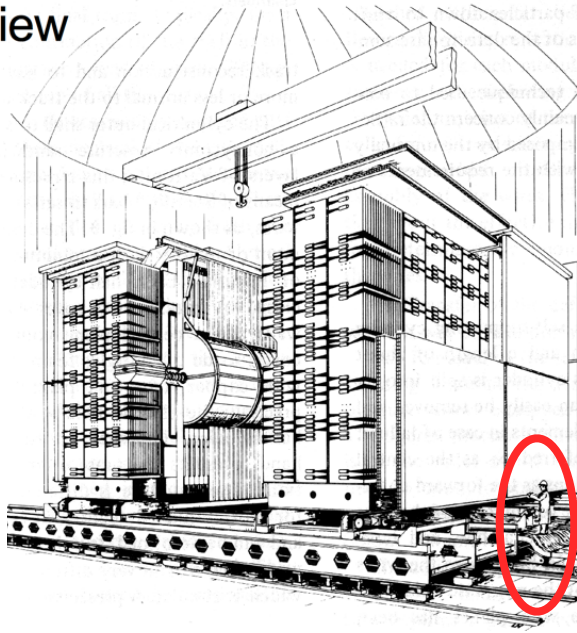
PFO Construction Algorithms



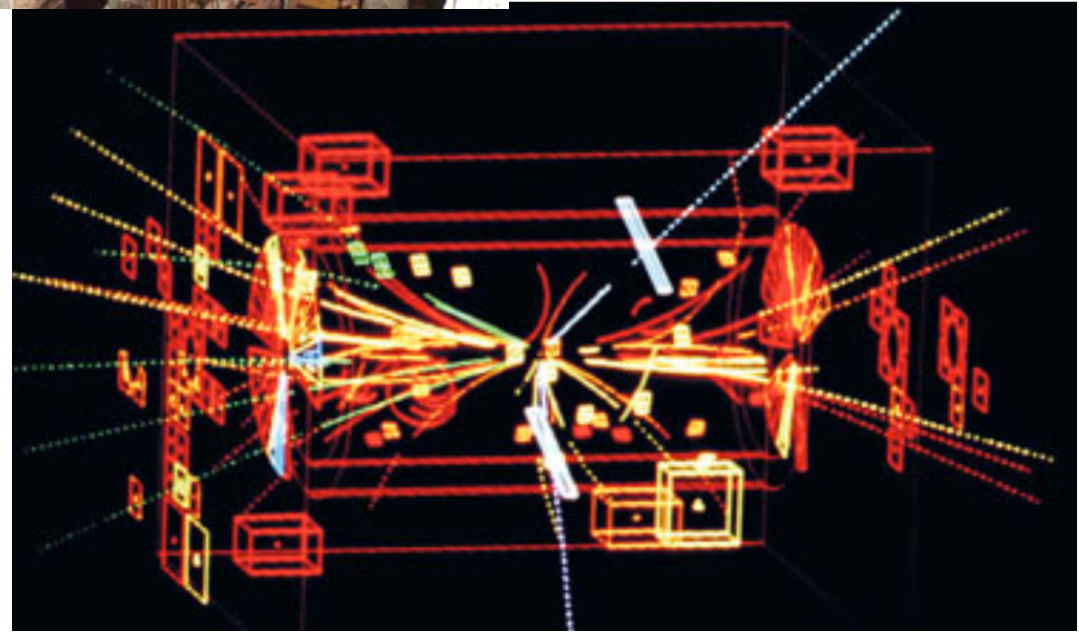
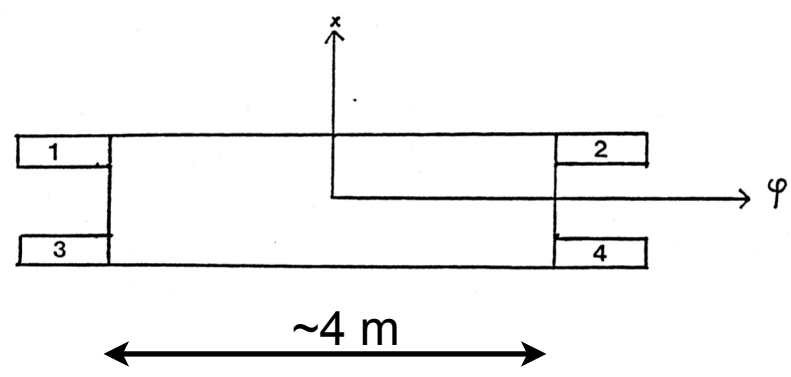
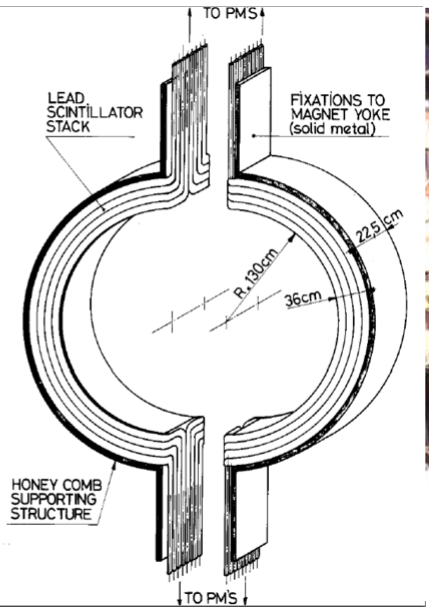
UA1 @ ppbar collider (1981): W/Z discovery

Design 1978-1980 - Built 1980-1982
 Operation 1982-1990

overview



electromagnetic calorimeter:
gondola



20x400 cm² - $\sigma/E \sim 0.15/\sqrt{E}$

ALEPH CALORIMETER: Z & WW studies

Design 1980-1982 - Built 1983-1988
 Operation 1989-2000

1 The Electromagnetic Calorimeter (ECAL)

Description: A sampling calorimeter, consisting of lead sheets and wire chambers, situated inside the solenoid. The barrel and two end-caps each comprise 12 modules and the longitudinal shower development is sampled in 45 layers grouped in three stacks of 10, 23 and 12 layers. The wire chambers are Al extrusion covered with graphite coated mylar. Signals are taken from cathode pads as well as from the anode wires. In each stack the pads form towers pointing to the interaction vertex. Gas: $XeCO_2$ (80% : 20%).

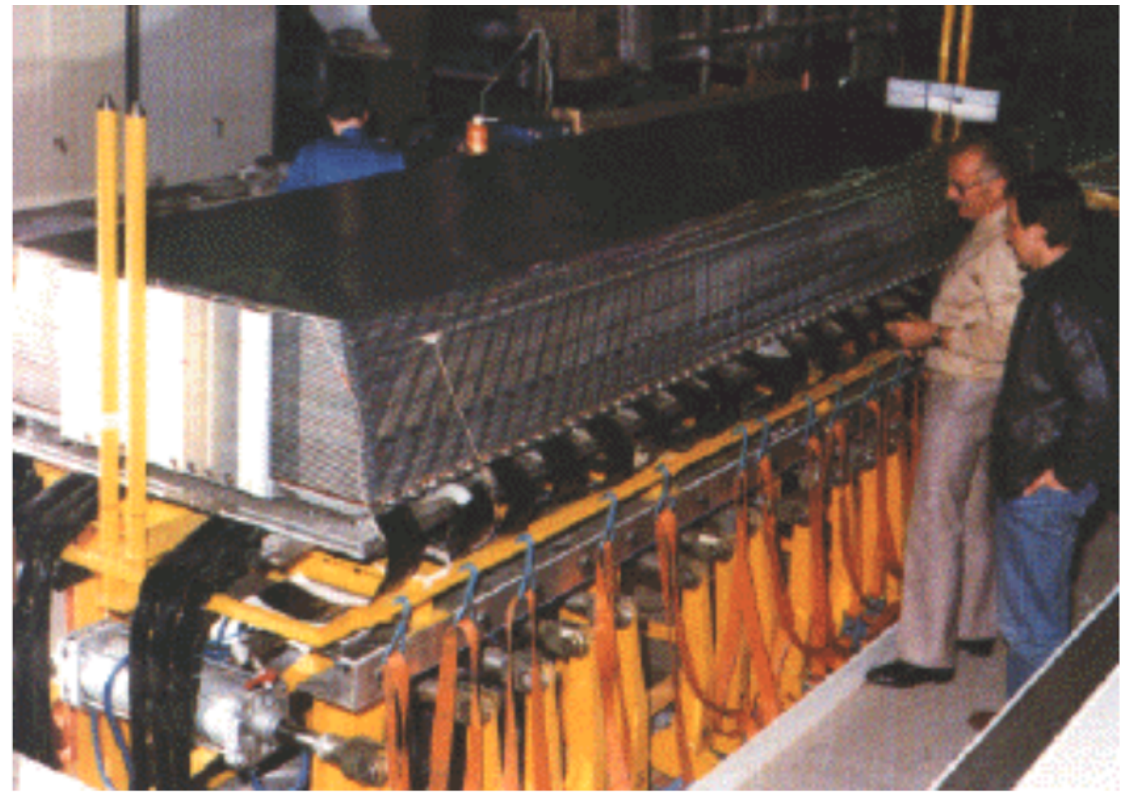
Dimensions: Thickness of lead plates 2 mm (stack 1+2), 4 mm (stack 3)
 Diameter of tungsten wire 25 μ
 Wire spacing 5 mm
 Radiation length/stack Barrel: $3.83X_0$, $8.80X_0$, $8.85X_0$
 Endcaps: $3.46X_0$, $8.86X_0$, $8.91X_0$
 8.91 X_0
 Interaction length 1.0 - 1.3 λ_{int} for 5GeV pions

Barrel:
 Radius: $R_{outer} = 225$ cm $R_{inner} = 185$ cm
 overall length 477 cm
 Weight per module 17 t (12 modules)
 Pad size at inner radius 3 cm \times 3 cm
 Granularity $\Delta\theta \times \Delta\phi \sin\theta$
 11 mrad \times 17 mrad at 90°
 12 mrad \times 12 mrad at 45°

Endcaps:
 Radius: $R_{outer} = 235.0$ cm $R_{inner} = 54.0$ cm
 Radius (active layers) $R_{outer} = 227.5$ cm $R_{inner} = 56.8$ cm
 Distance from I.P. 250.5 cm active layer: 255.0 cm
 Overall length (each) 56.25 cm active layers: 41.10 cm
 Weight per module 2.6 t (2 \times 12 modules)
 Granularity $\Delta\theta \times \Delta\phi \sin\theta$
 12 mrad \times 14 mrad for $11^\circ < \theta < 16^\circ$
 11 mrad \times 12 mrad for $16^\circ < \theta < 27^\circ$
 10 mrad \times 11 mrad for $27^\circ < \theta < 36^\circ$
 10 mrad \times 10 mrad for $36^\circ < \theta < 42^\circ$

Readout: Channels:
 Tower storeys = $12 \times 3 \times 4,096$ (barrel) + $2 \times 12 \times 3 \times 1,024$ (endcap) = 221,184 (total)

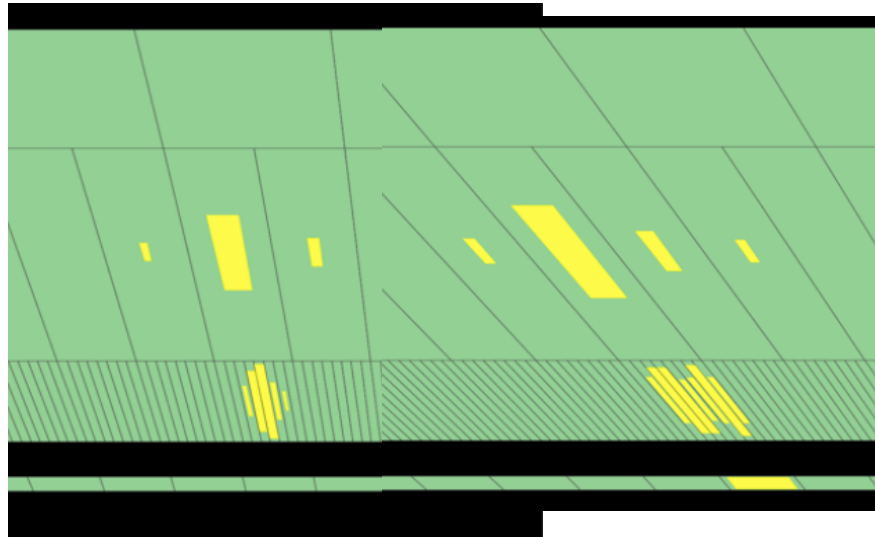
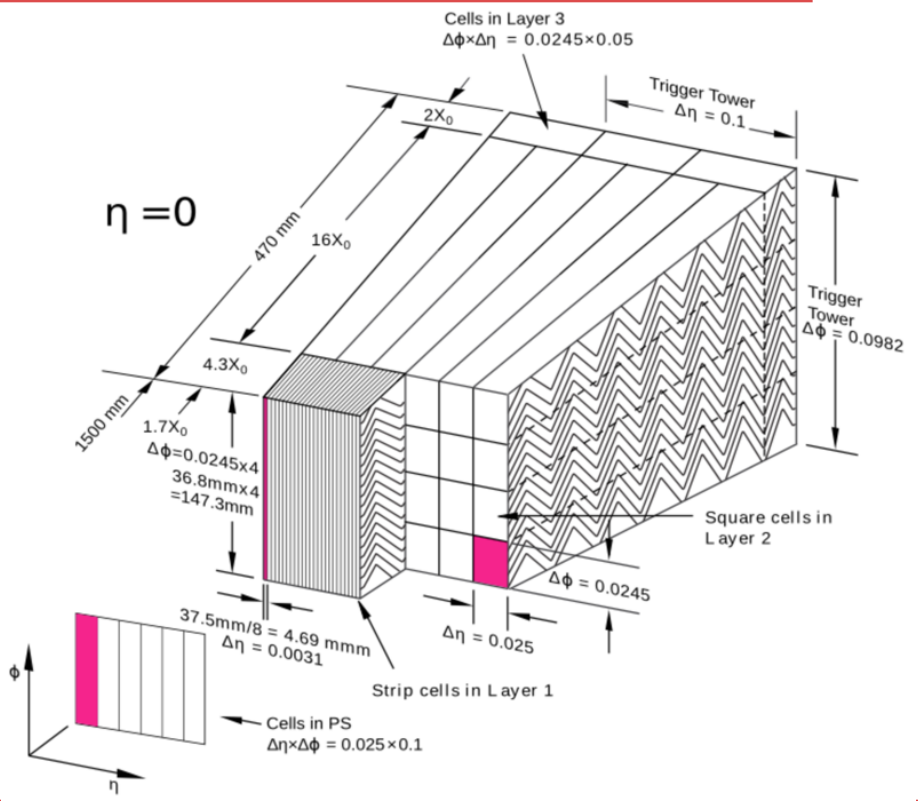
Performance: Energy resolution $\sigma/E = 0.01 + 0.18/\sqrt{E(GeV)}$
 Angular resolution $\sigma_\theta = \sigma_\theta / \sin\theta = 0.02 + 2.5/\sqrt{E(GeV)}$ mrad



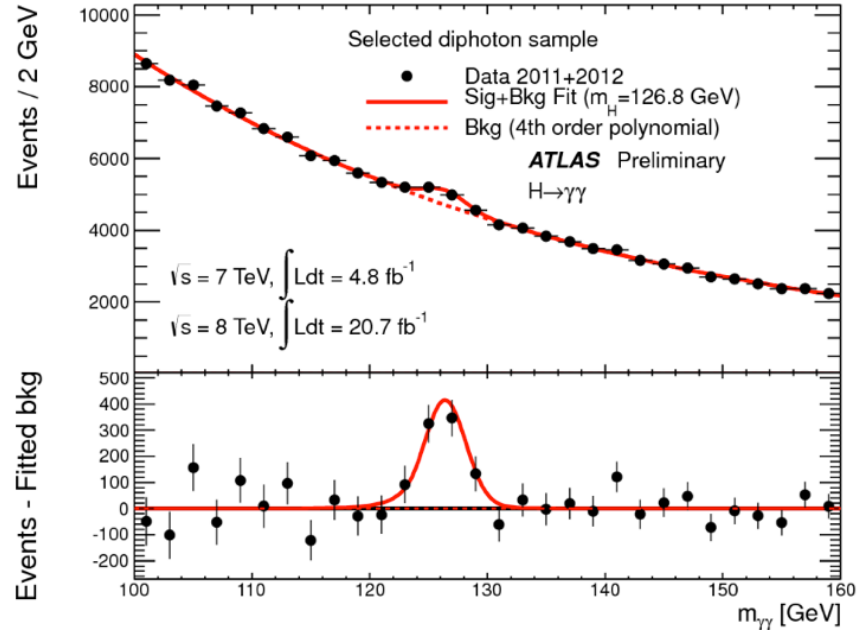
3×3 cm² - $\sigma/E \sim 0.18/\sqrt{E}$

ATLAS CALORIMETER: HIGGS BOSON DISCOVERY

Design 1997-2000 - Built 2001-2004
 Operation 2007-2035 ?



LAr 182428 channels $|\eta| < 4.9$ ($\theta > 0.6^\circ$)
EM $\Delta\eta \times \Delta\phi = 0.025 \times 0.1 / 0.003 \times 0.1 / 0.025 \times 0.025 / 0.05 \times 0.025$
HAD $\Delta\eta \times \Delta\phi = 0.1 \times 0.1 / 0.2 \times 0.2$
FCal $\Delta x \times \Delta y \approx 2 \times 2 \text{ cm}^2$
Tiles 9836 channels $|\eta| < 1.7$
 28th June-4th July 2017 $\Delta\eta \times \Delta\phi = 0.1 \times 0.1$



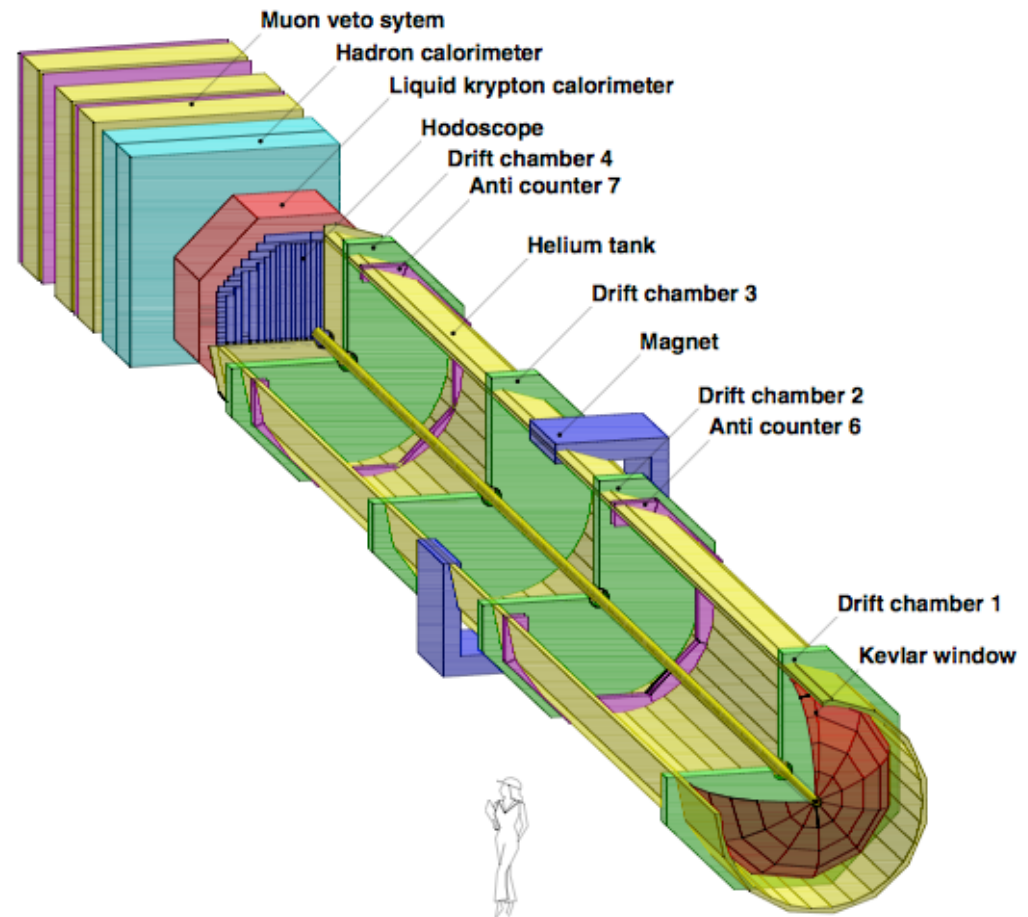
$0.8 \times 16 \text{ cm}^2$ & $4 \times 4 \text{ cm}^2$
 $\sigma/E \sim 0.10/\sqrt{E}$

THE NA48 EXPERIMENT

NA48 experiment started data taking in 1997

Now the NA62 experiment, searching for rare Kaon decays is starting data taking with the SAME calorimeter using Liquid Krypton.

The calorimeter has not been warmed up since 1998.



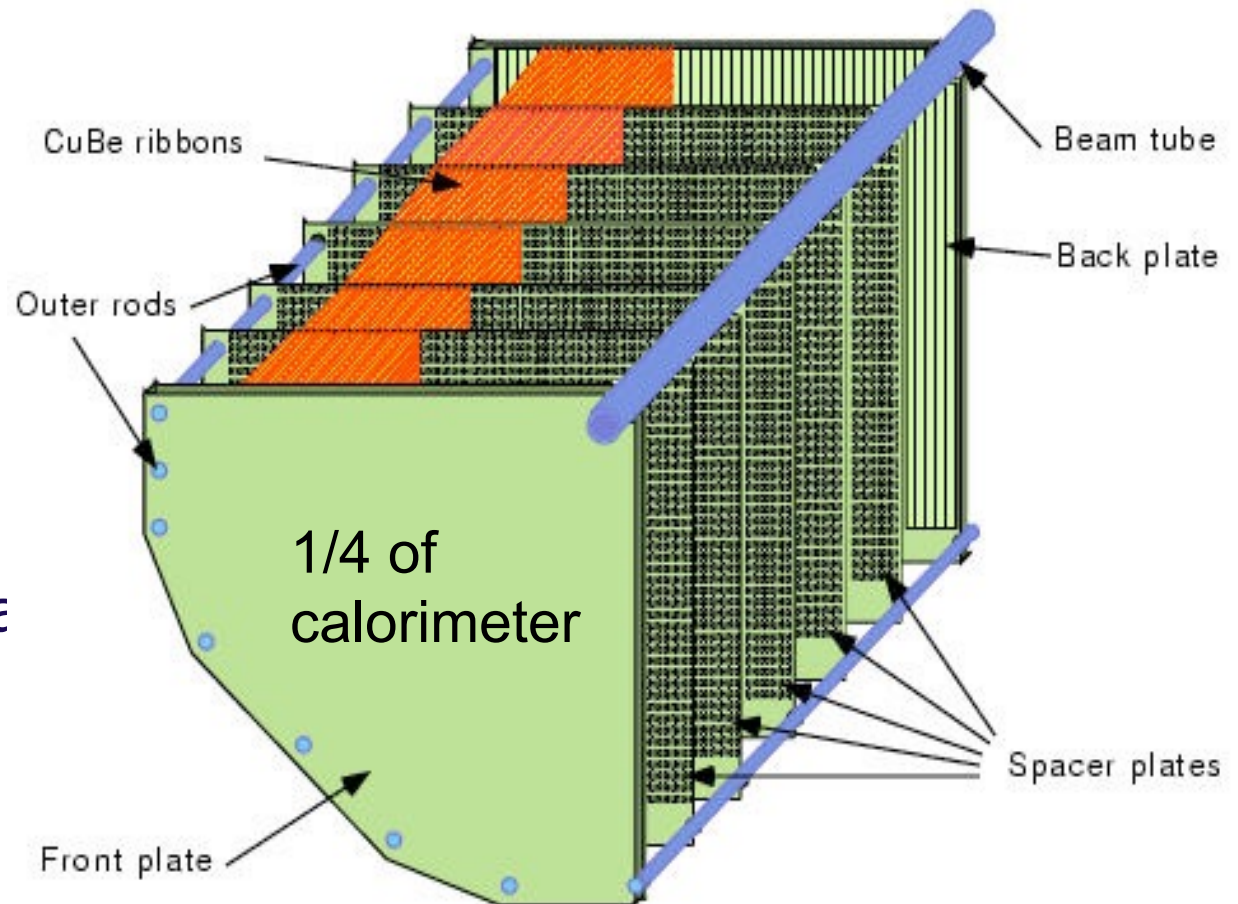
◆ $K_{L,S} \rightarrow \pi^+ \pi^-$

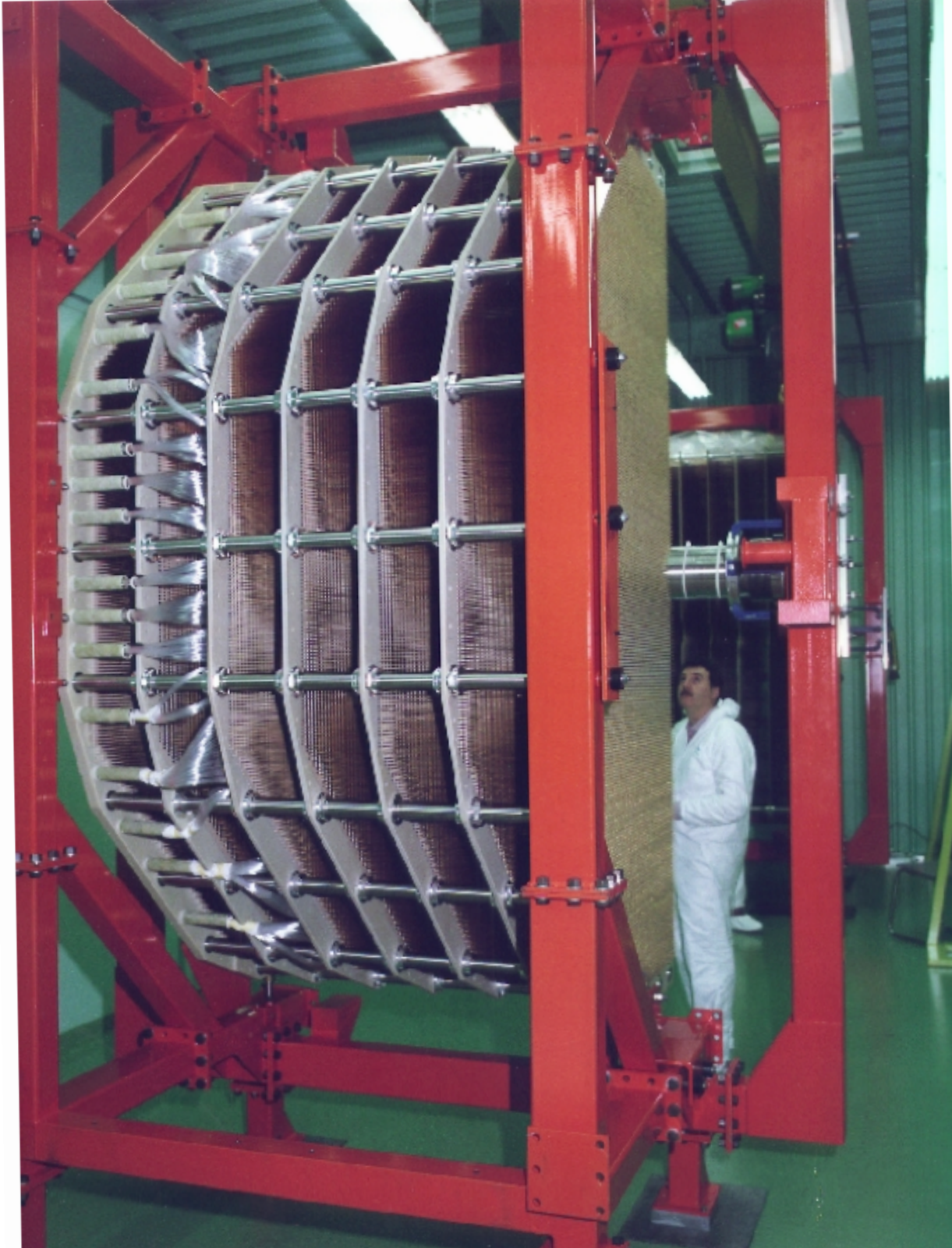
- **Magnetic spectrometer** ($\sigma_{X,Y} \sim 90 \mu\text{m}$)
- $\sigma(P)/P \simeq 0.5 \% \oplus 0.009 P[\text{GeV}/c] \%$ ($\sim 1 \%$ for 100 GeV/c track momentum)
- **Hodoscope** for timing measurements ($\sigma_t \sim 200 \text{ps}$)
- **Muon veto** to reject $\pi\mu\nu$ background.

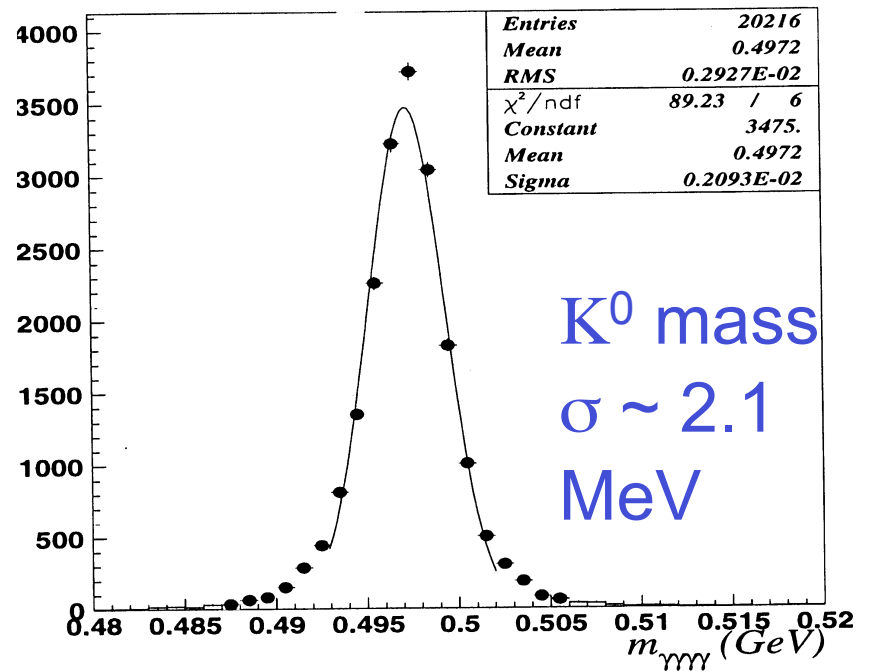
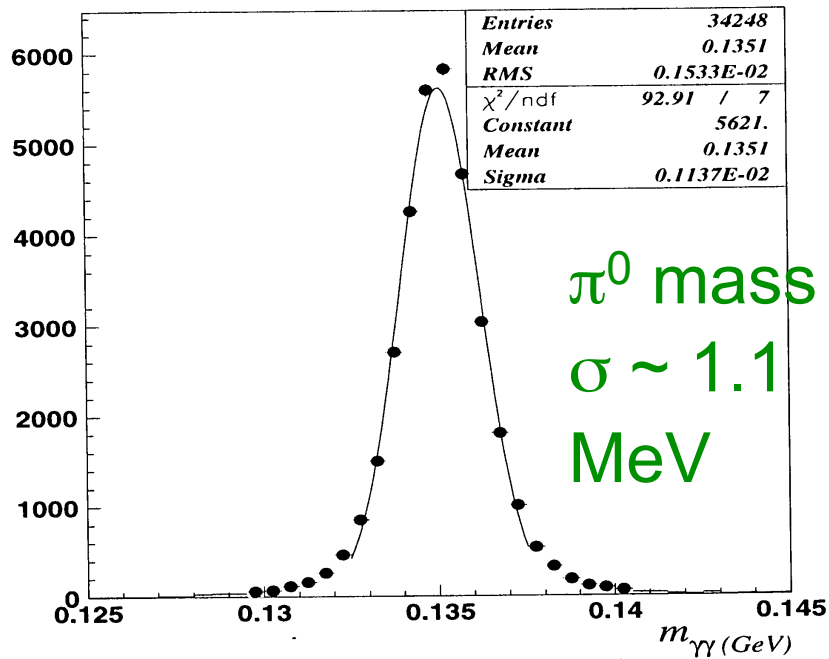
NA48 LIQUID KRYPTON ELECTROMAGNETIC CALORIMETER: HOMGENUOUS CALORIMETER

- NA48 has measured $\text{Re}(\epsilon'/\epsilon)$
 $\sim 10^{-4}$ by identifying the mode
 $K_S \rightarrow \pi^0 \pi^0$ and $K_L \rightarrow \pi^0 \pi^0 \pi^0$
- Good resolution on $m(\pi^0)$
necessary: 1MeV
- ($m(\pi^0) = 135\text{MeV}$)
- Energy resolution $5\%/\sqrt{E}$
- LKr bath instrumented with
electrodes with a zig-zag shape

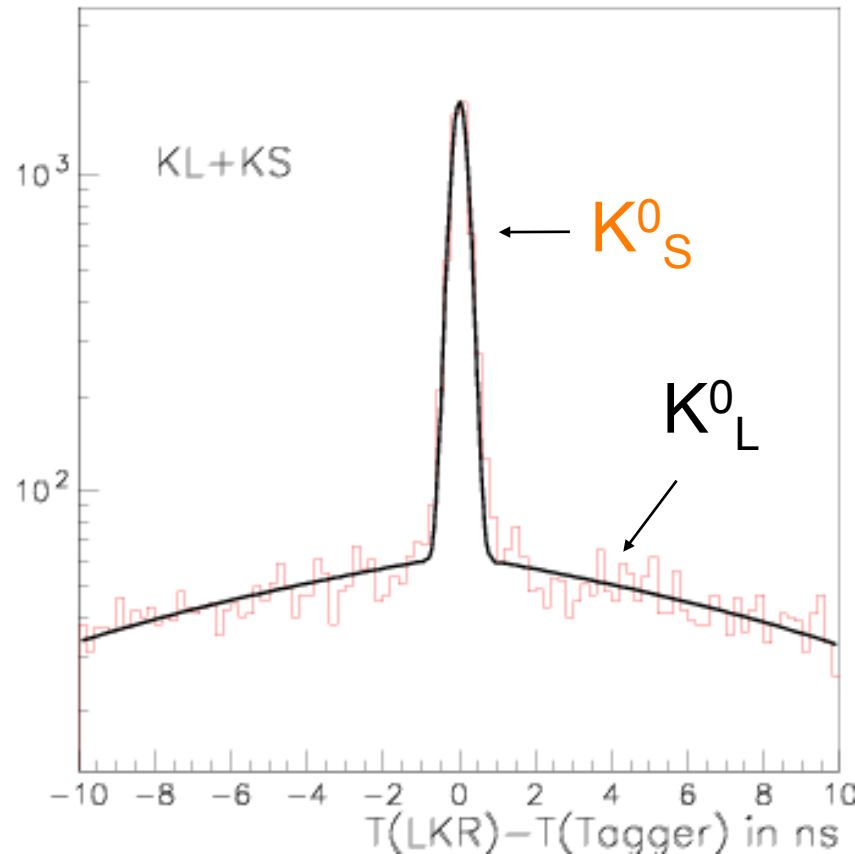
Liquid Krypton $T = 120 \text{ }^\circ\text{K}$







NA48



Calorimeter
 time resolution
 $\sigma \sim 220$ ps

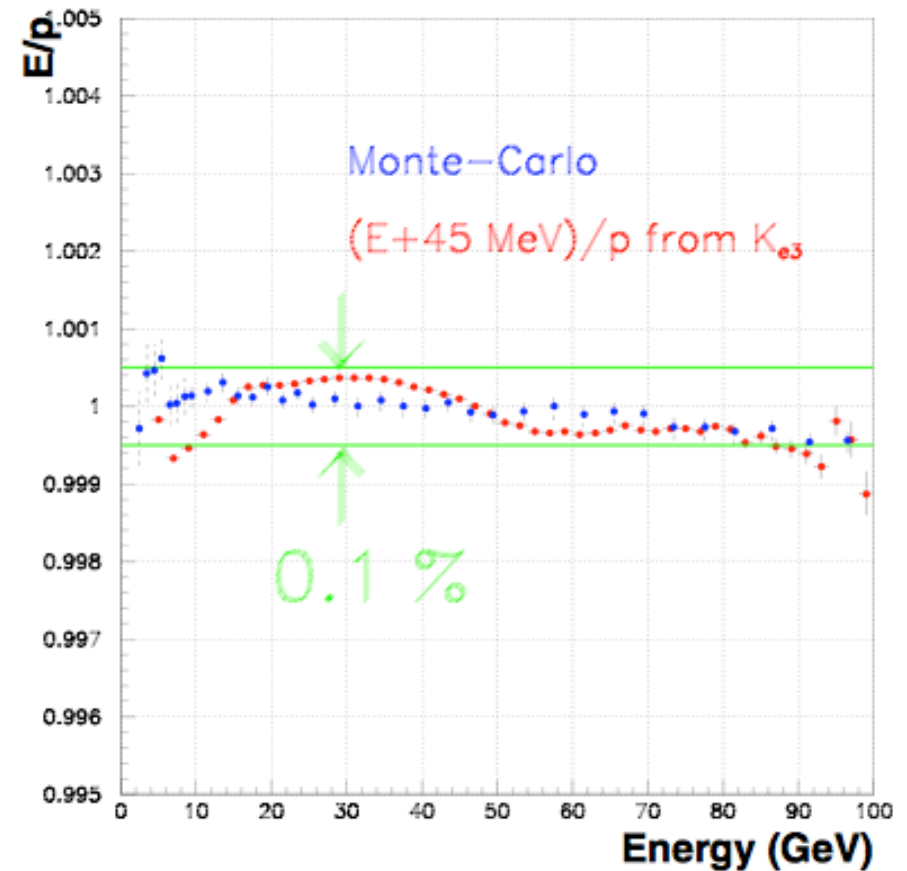
ENERGY LINEARITY

ENERGY RESPONSE LINEARITY is
CRITICAL for MASS MEASUREMENT

In NA48, study the calorimeters in-situ selecting
 $K_L \rightarrow \pi^\pm e^\mp \nu$ decays

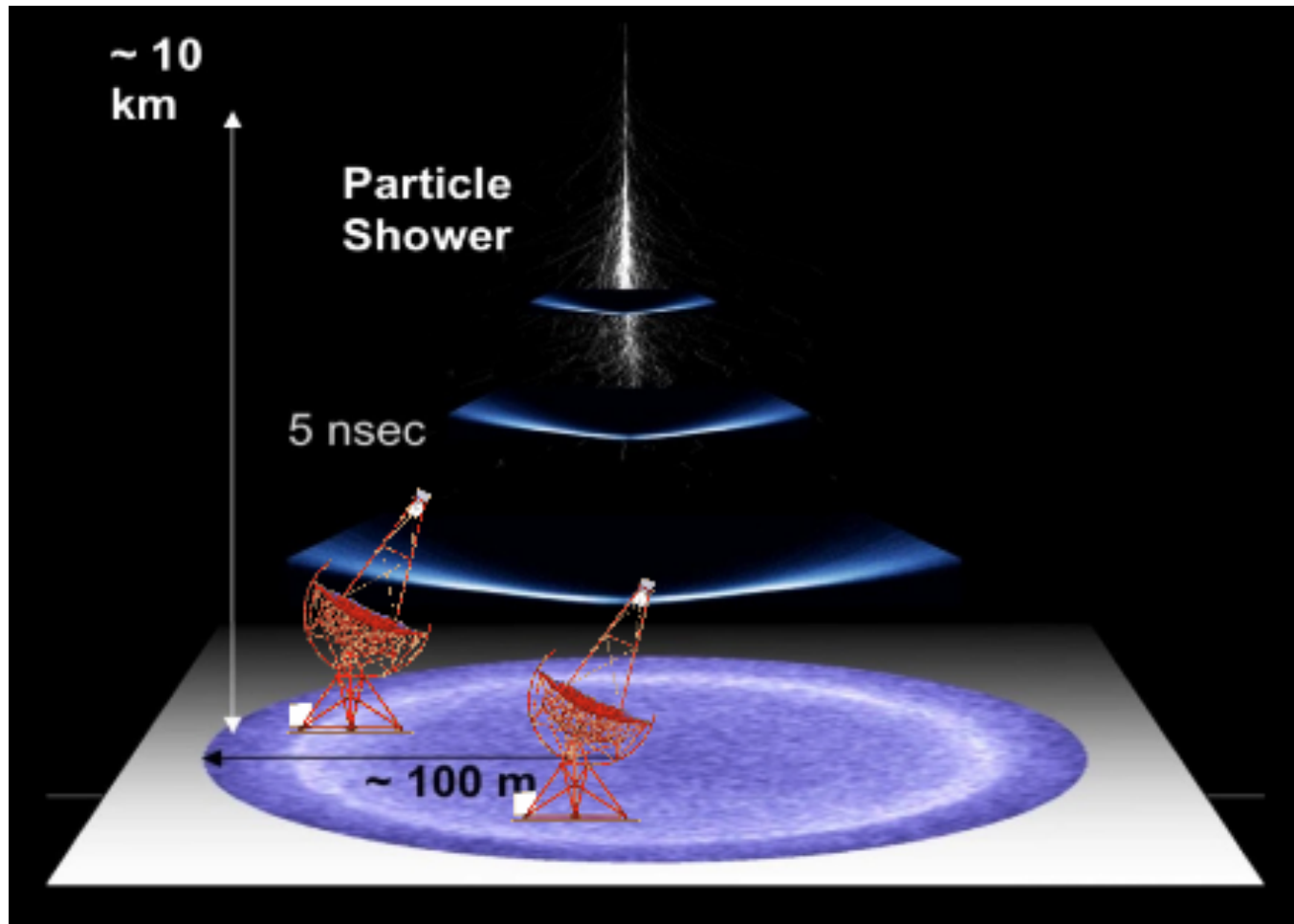
Use the spectrometer to measure p (resolution
 $\sim 0.5\text{-}1\%$)
and the calorimeter to measure E

In an ideal world: $E/p=1$

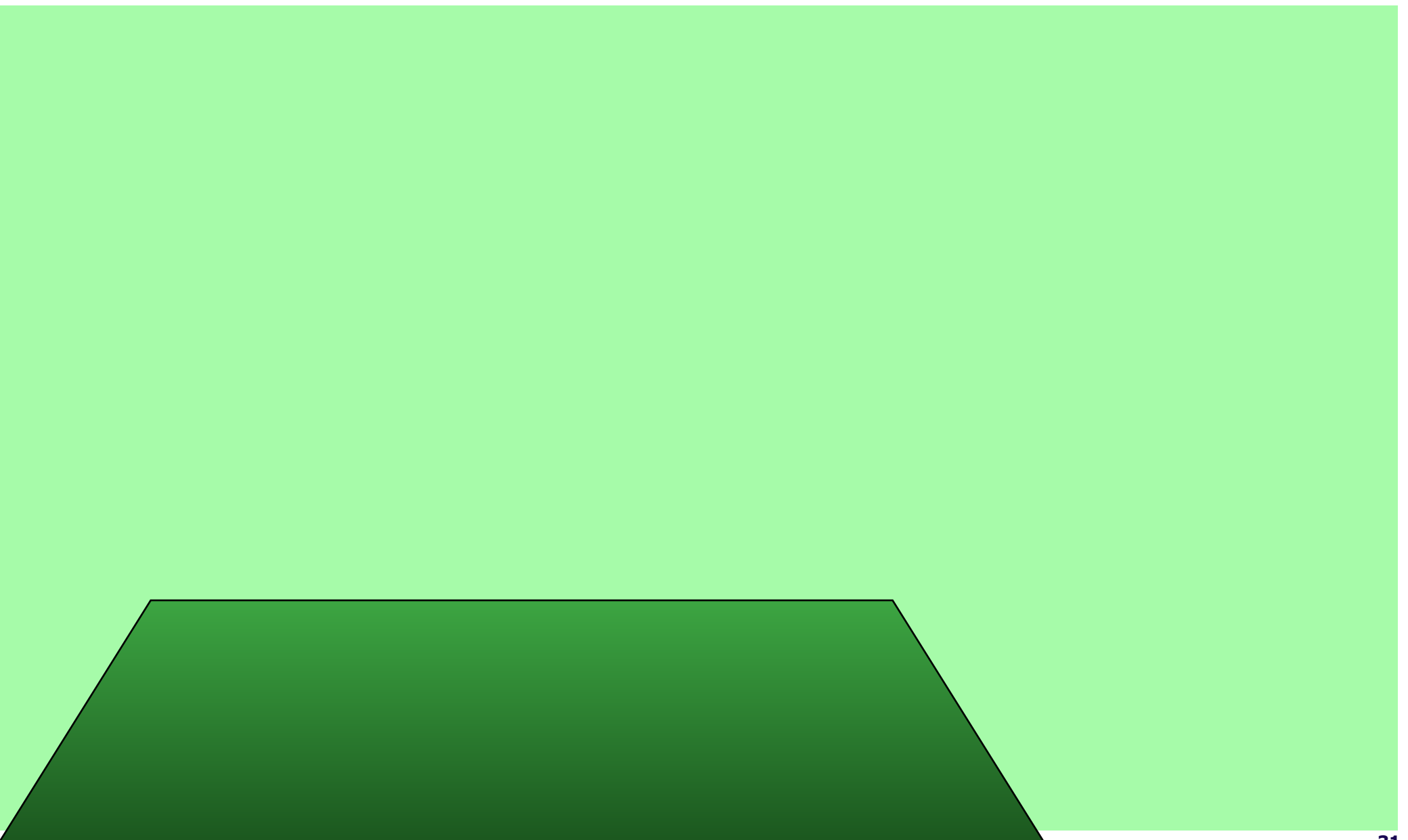


\Rightarrow Non linearity $\approx 0.1\%$
(from 5 to 100 GeV)

NATURAL CALORIMETER

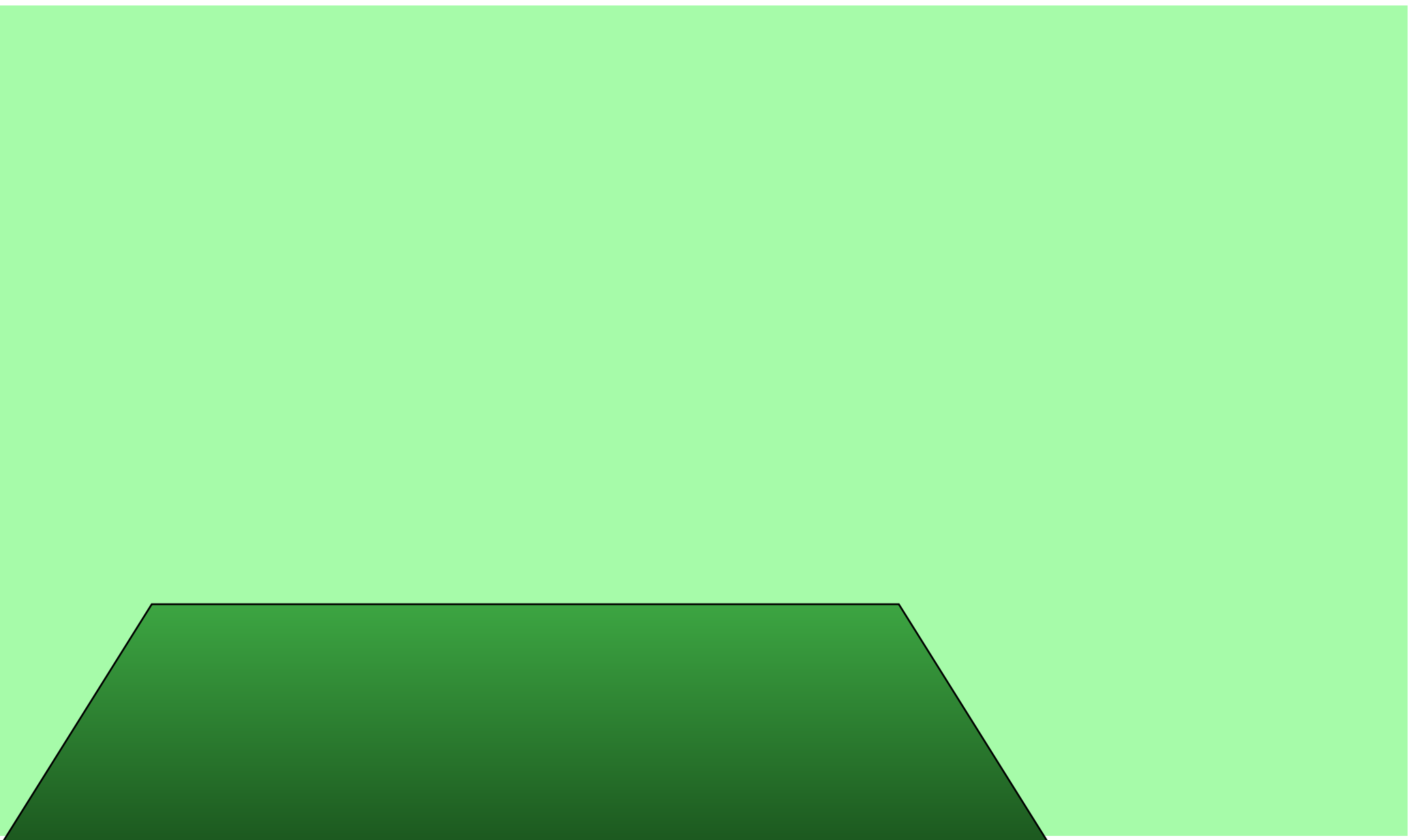


Air CALORIMETER: High Energy Stereoscopic System



Air CALORIMETER: High Energy Stereoscopic System

Gamma
ray



Air CALORIMETER: High Energy Stereoscopic System

Gamma
ray

Air shower

~ 10 km

Air CALORIMETER: High Energy Stereoscopic System

Gamma ray

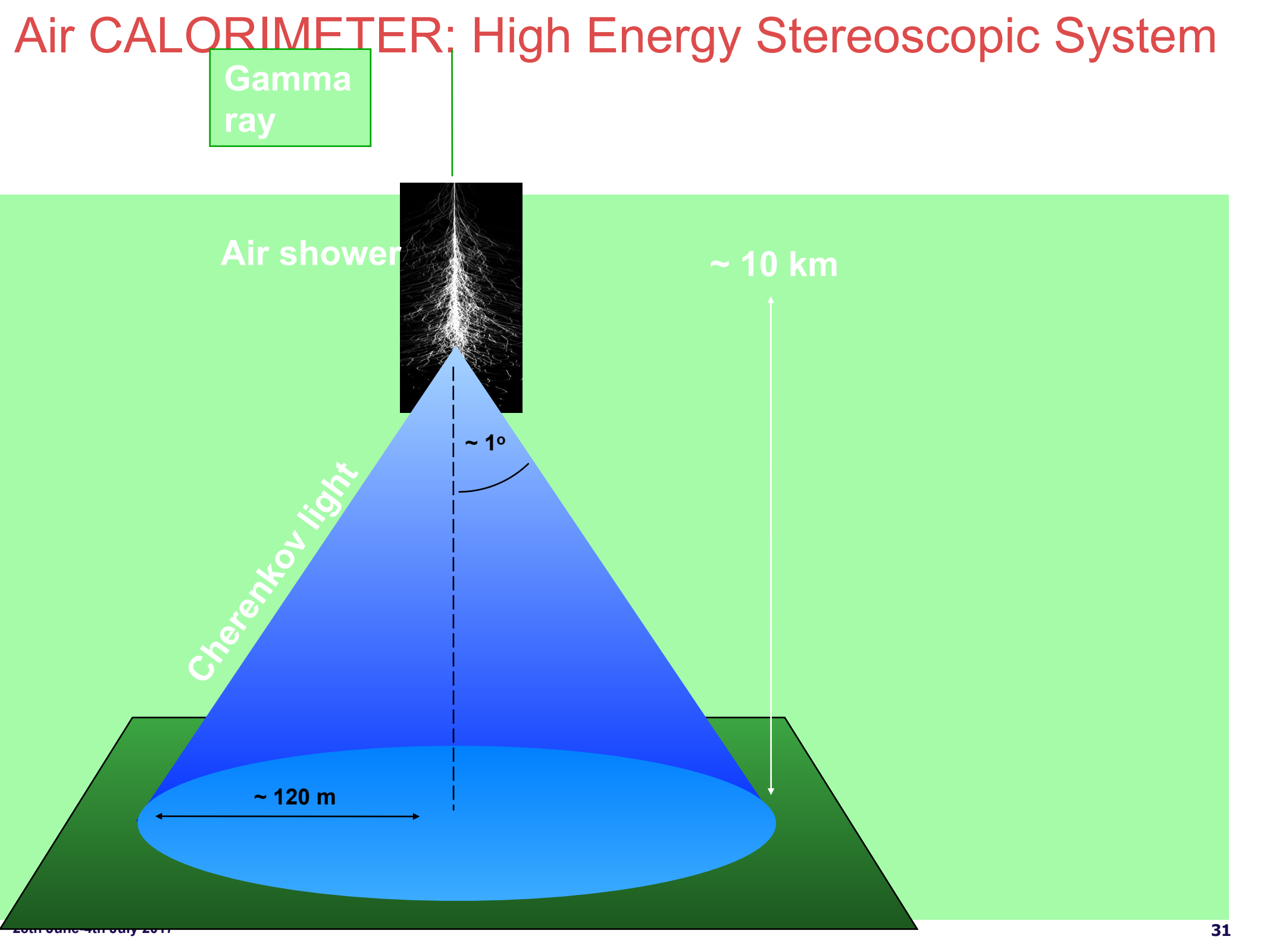
Air shower

~ 10 km

Cherenkov light

~ 1°

~ 120 m



Air CALORIMETER: High Energy Stereoscopic System

Gamma ray

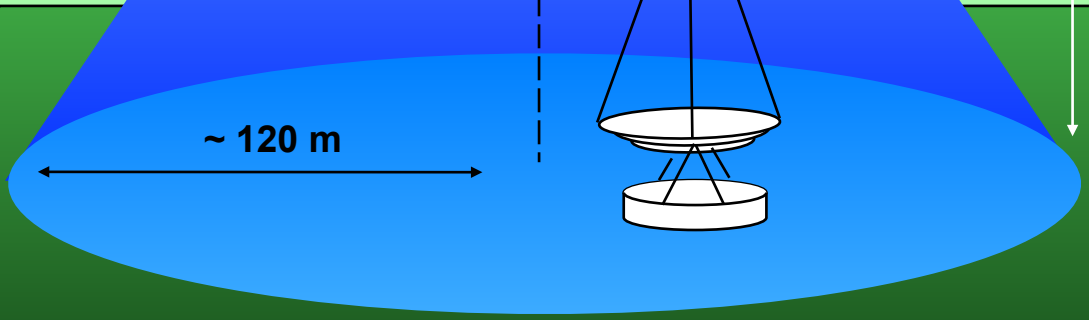
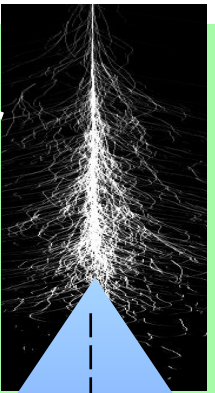
Air shower

~ 10 km

Cherenkov light

~ 1°

~ 120 m



Air CALORIMETER: High Energy Stereoscopic System

Gamma ray

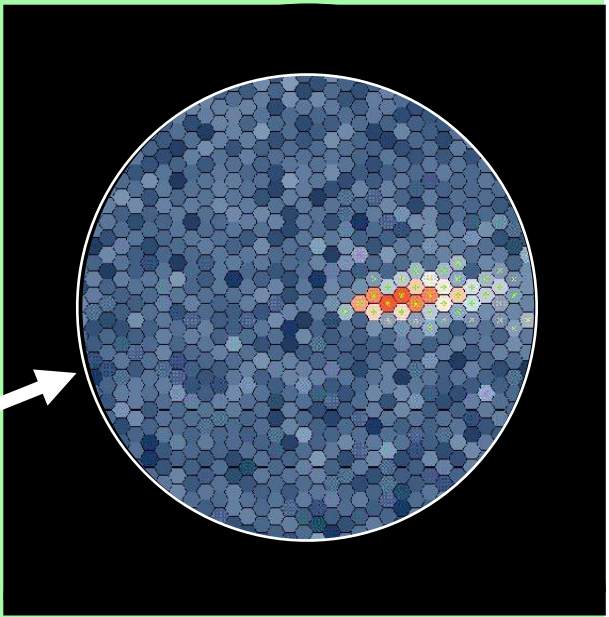
Air shower

~ 10 km

Cherenkov light

1°

~ 120 m



Air CALORIMETER: High Energy Stereoscopic System

Gamma ray

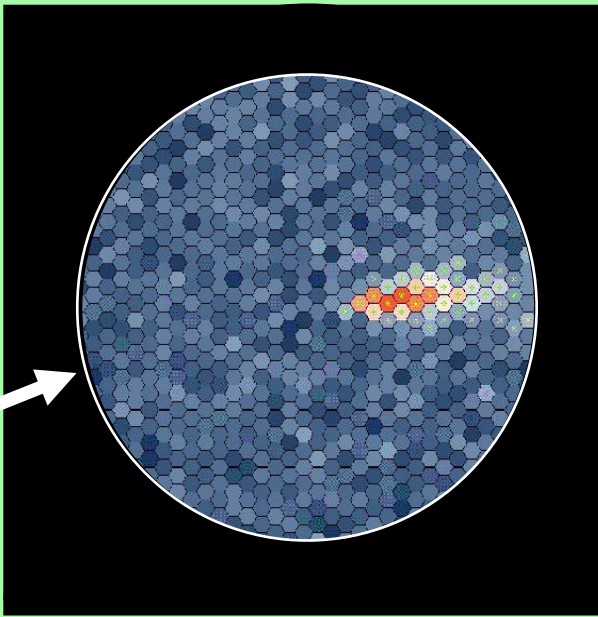
Air shower

~ 10 km

Cherenkov light

1°

~ 120 m



Air CALORIMETER: High Energy Stereoscopic System

Gamma ray

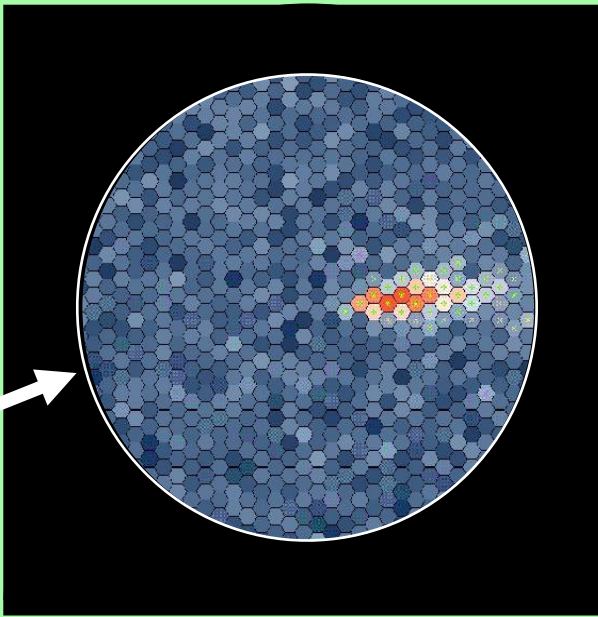
Air shower

~ 10 km

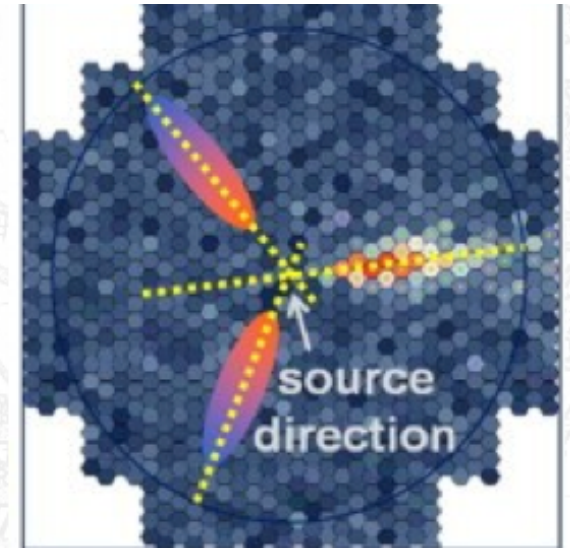
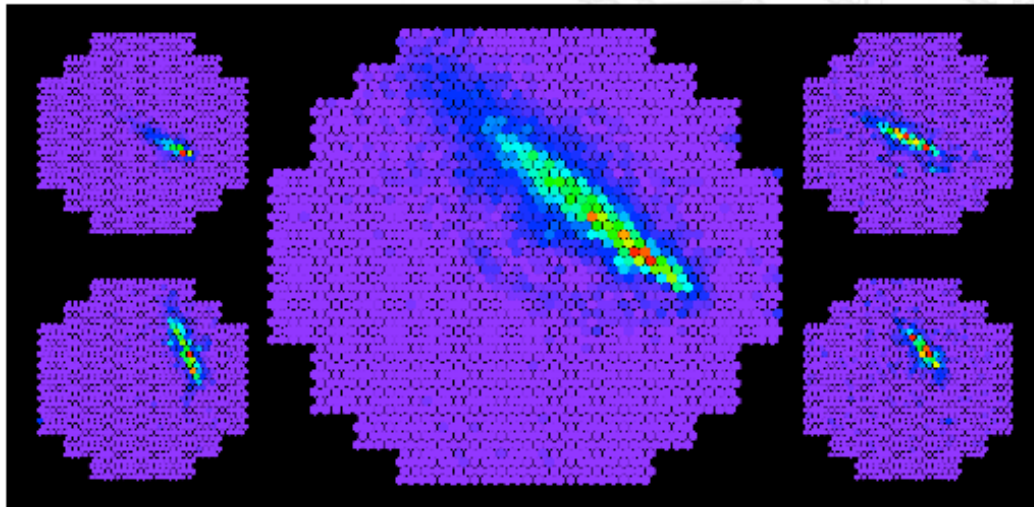
Cherenkov light

1°

~ 120 m

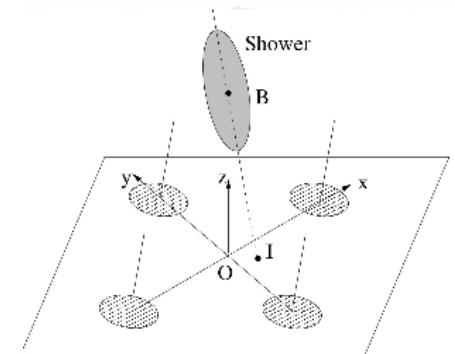


THE METHOD



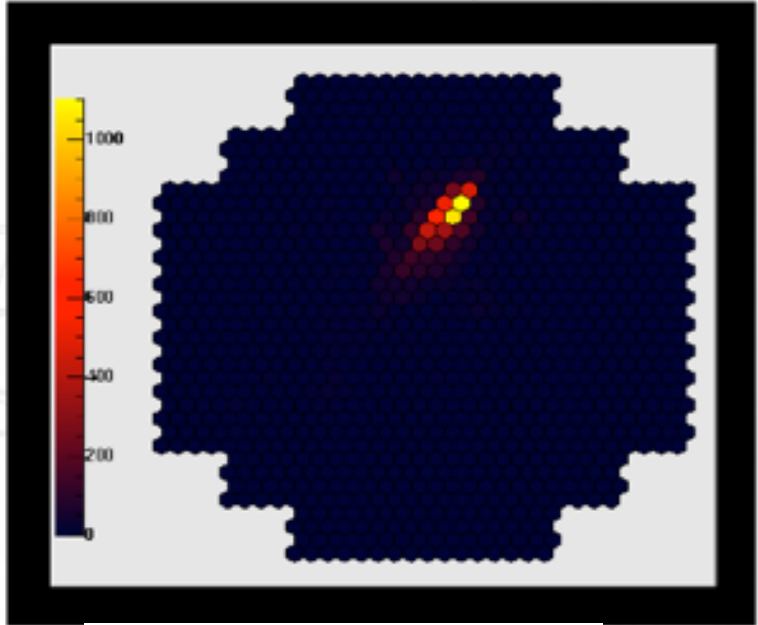
Reconstruct the shower position in atmosphere
Estimate the energy from signal in telescopes + simulation of air showers

Analyse Model 3D

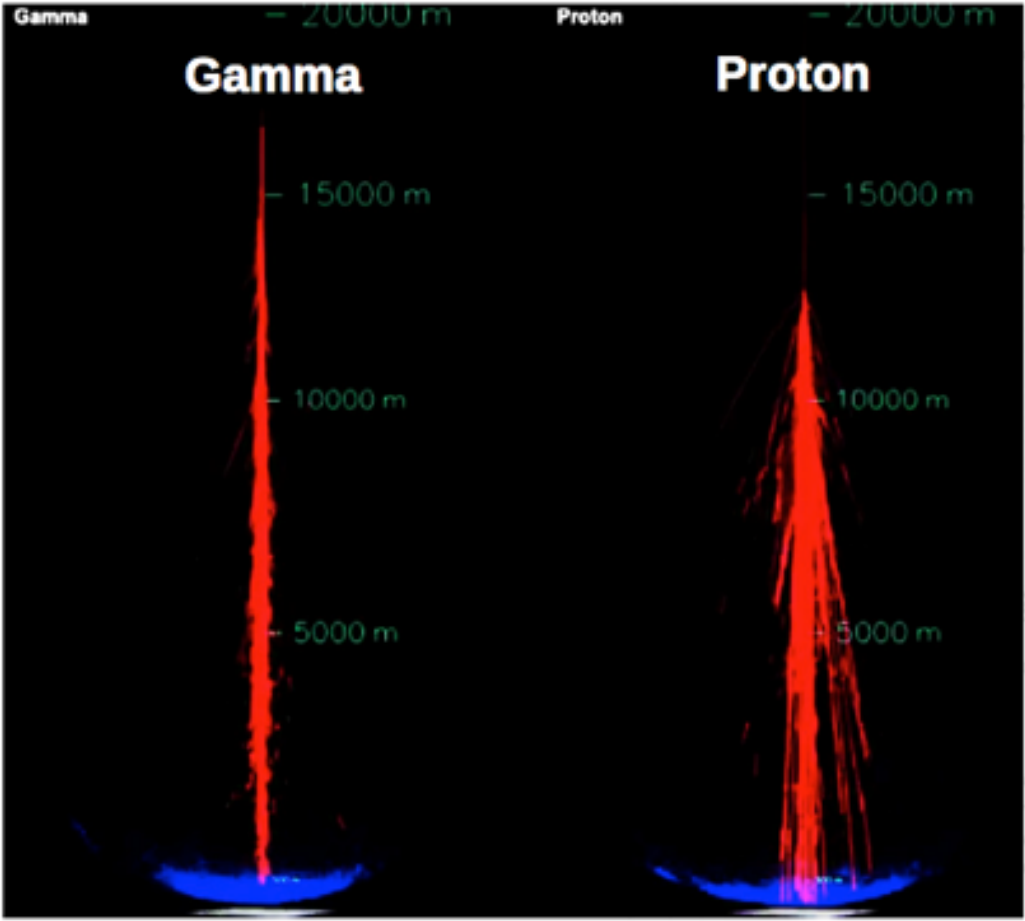
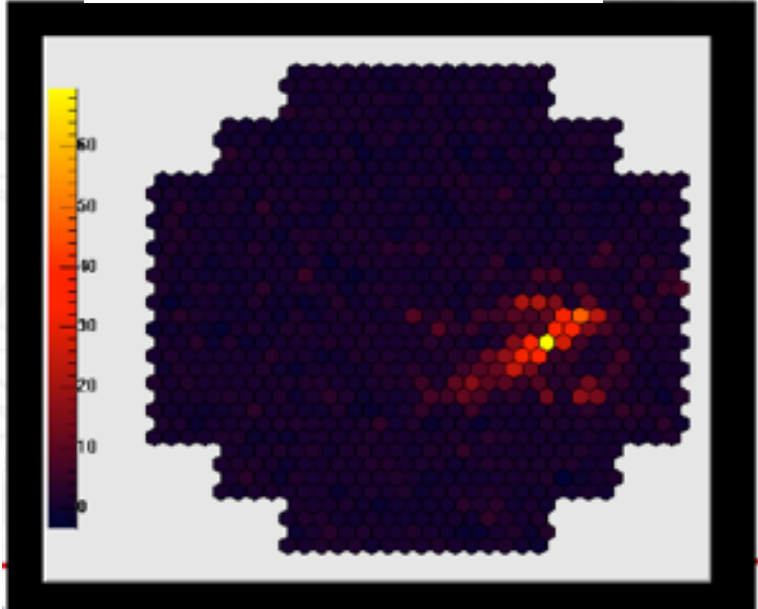


GAMMA RAYS DETECTIONS & SHOWER SHAPES

ELECTROMAGNETIC SHOWER



HADRONIC SHOWER

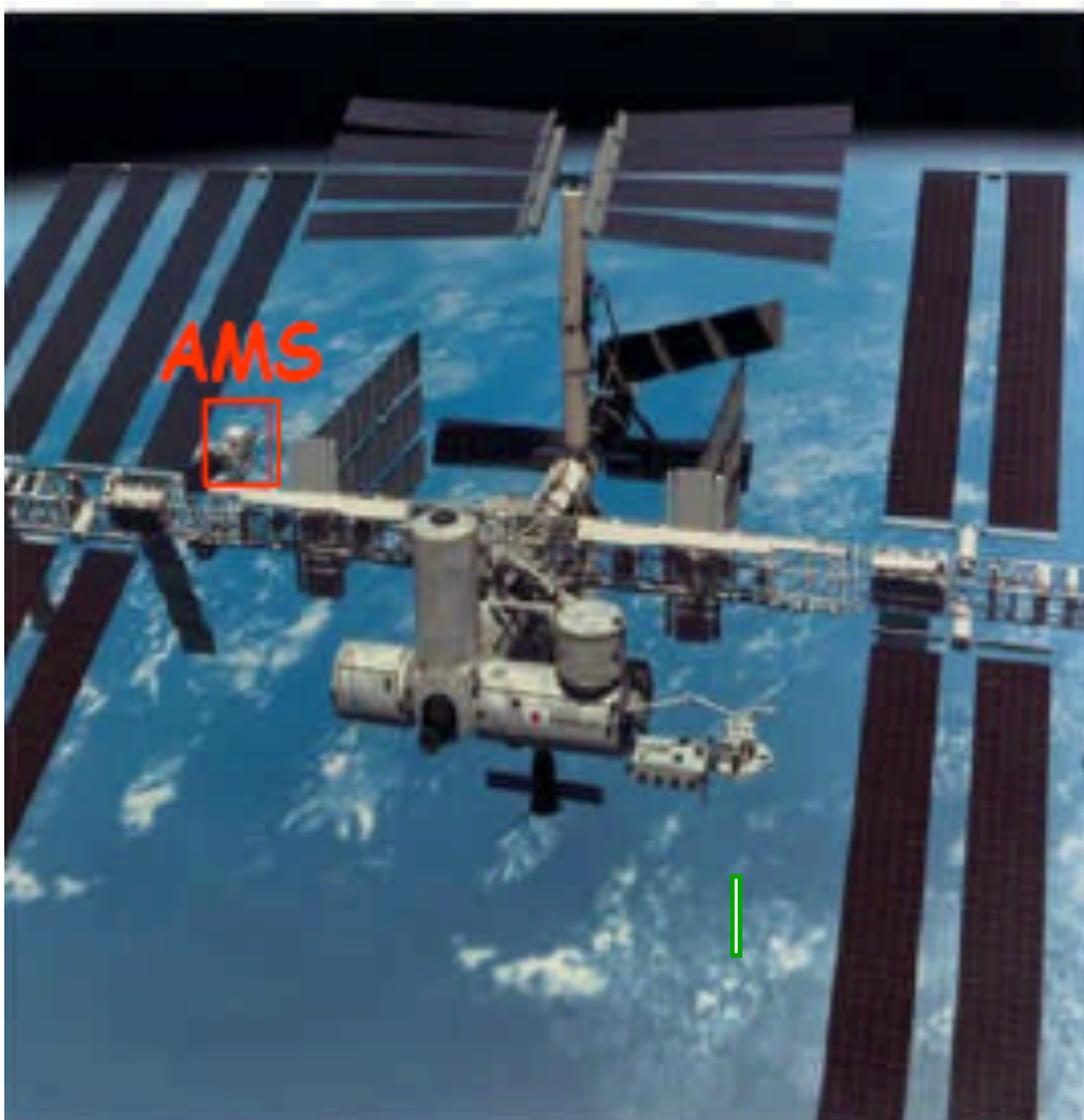


HESS EXPERIMENT INSTALLED in NAMIBIA



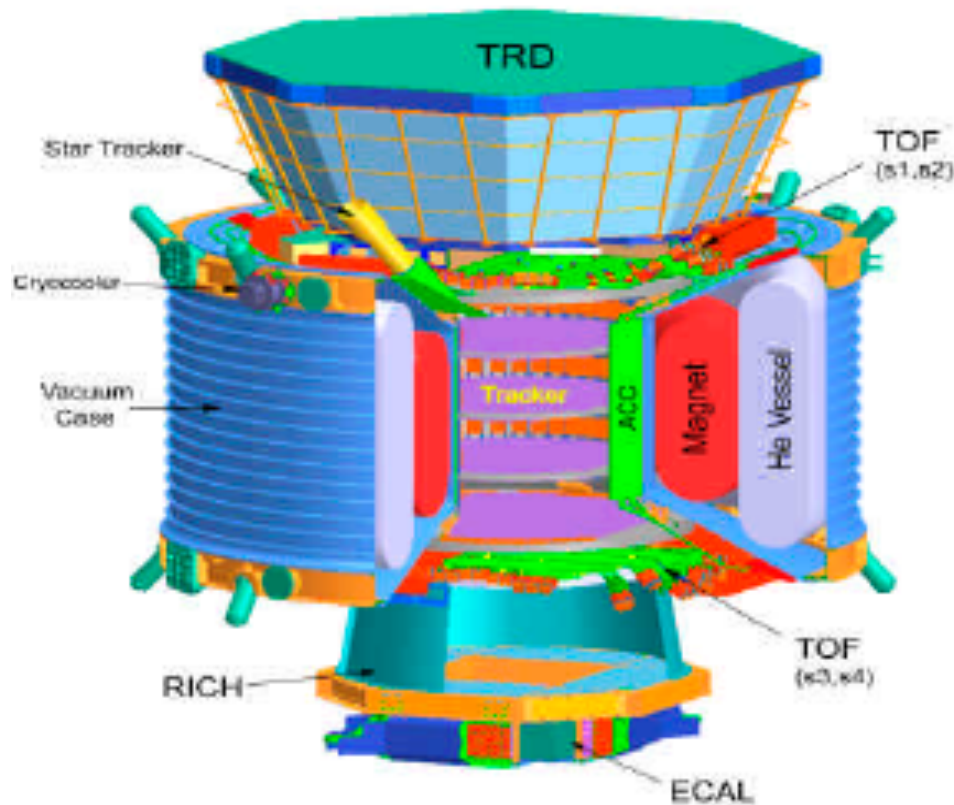
H.E.S.S.

ALPHA MAGNETIC SPECTROMETER



- AMS is designed to measure high energy cosmic rays.
- AMS is in particular searching for anti-matter (anti-He)
- AMS is a multi purpose particle detector in space.

AMS DETECTOR



AMS on ISS for 3 years

Transition Radiation Detector

Foam + drift tubes (Xe/CO₂)

Time of Flight (trigger)

Scintillators, fine mesh PMT's

$$\sigma_t \sim 120 \text{ ps}$$

Superconducting magnet (0.86 T·m²)

Tracker (8 layers, 6m²)

6 double-sided silicon strips

$$\sigma_x = 10 \text{ } \mu\text{m in bending plane}$$

RICH

Radiator (Aerogel+NaF)

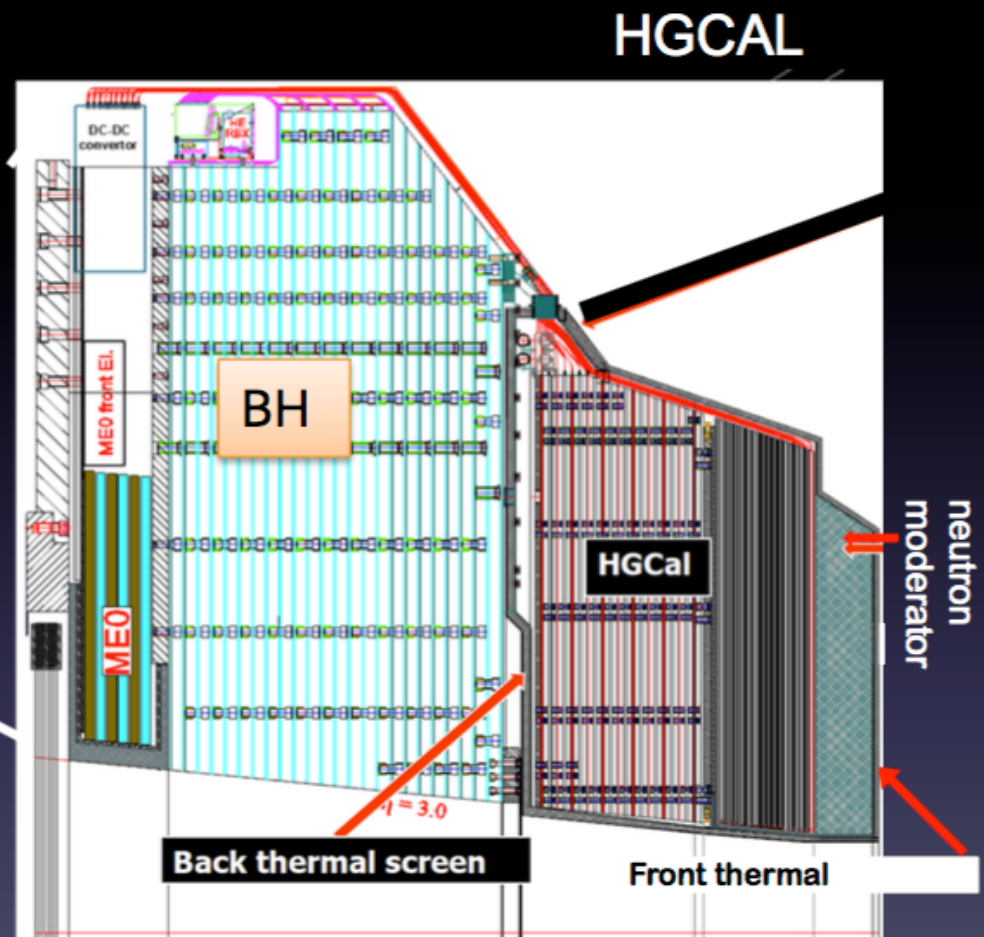
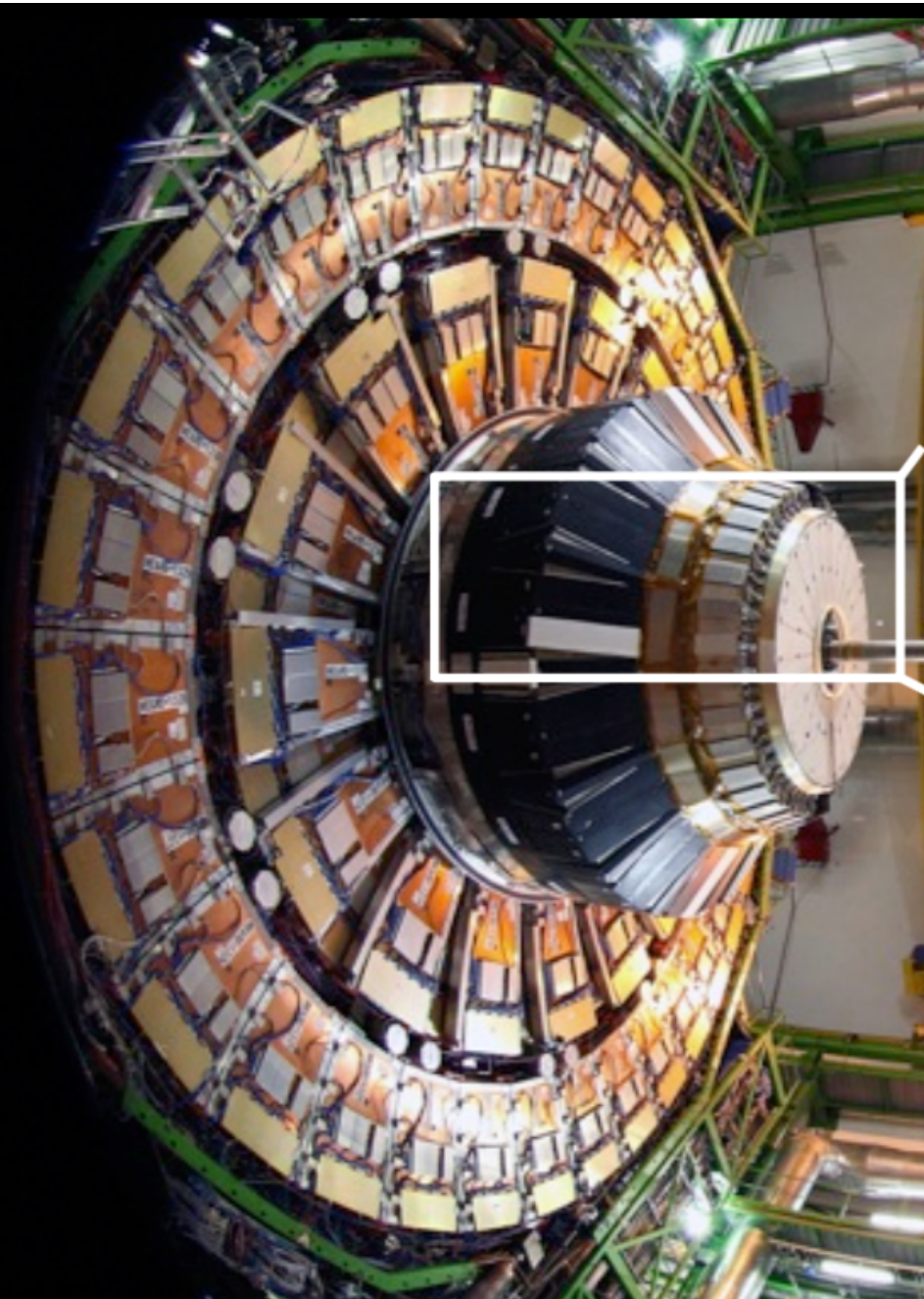
PMT's (16 pixels)

3D-sampling ECAL

Lead+Scintillating-fibers

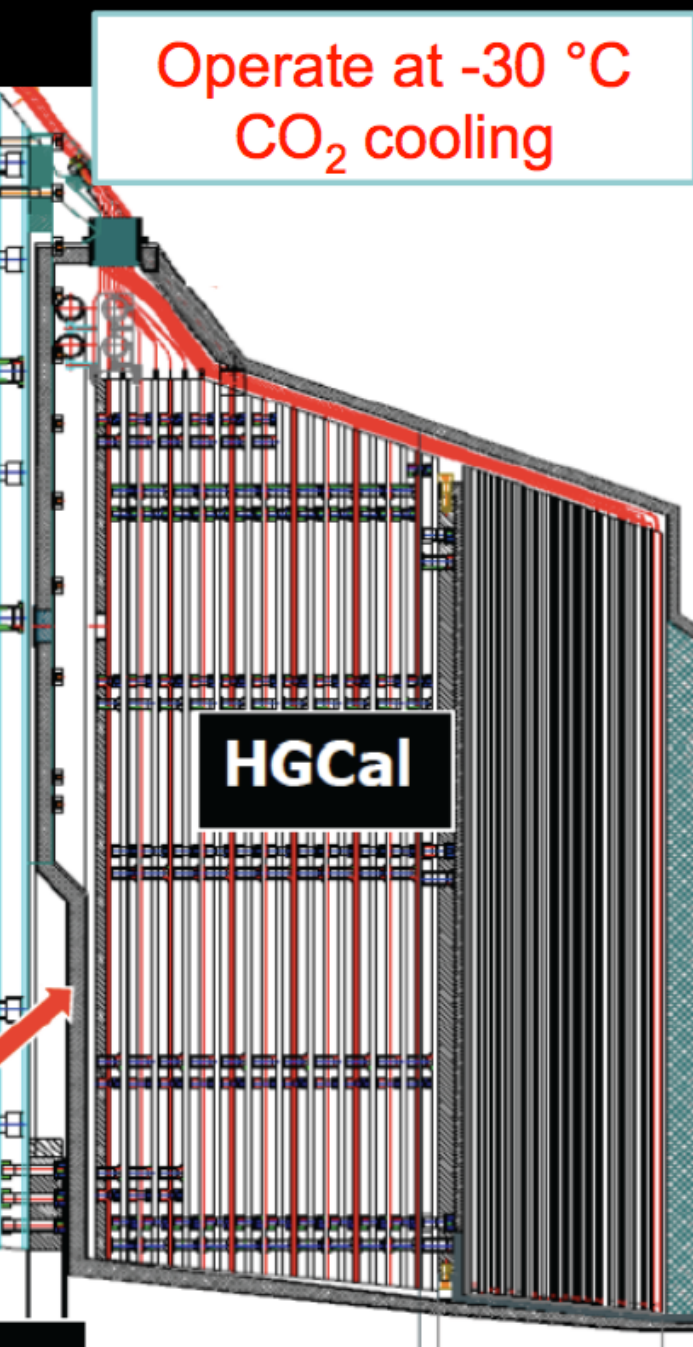
PMT's (4 pixels)

THE FUTURE of the CMS ENDCAP CALORIMETER



EE	Cu-W / Si	$26 X_0$ (1.5λ)
FH	Brass / Si	3.5λ
BH	Brass / scint. tiles	5λ

IMAGINING CALORIMETER



Operate at $-30\text{ }^{\circ}\text{C}$
 CO_2 cooling

Si/W-ECAL Section ($\Sigma_{\text{depth}} > 25X_0, 1.5\lambda$)

$10 \times 0.65X_0$

$10 \times 0.88X_0$

$8 \times 1.26X_0$

Si/Brass Front HCAL (FH) Section ($\Sigma_{\text{depth}} > 3.5\lambda$)

$12 \times 0.3\lambda$

Scint/Brass Backing HCAL (BH) Section ($\Sigma_{\text{depth}} > 5\lambda$)

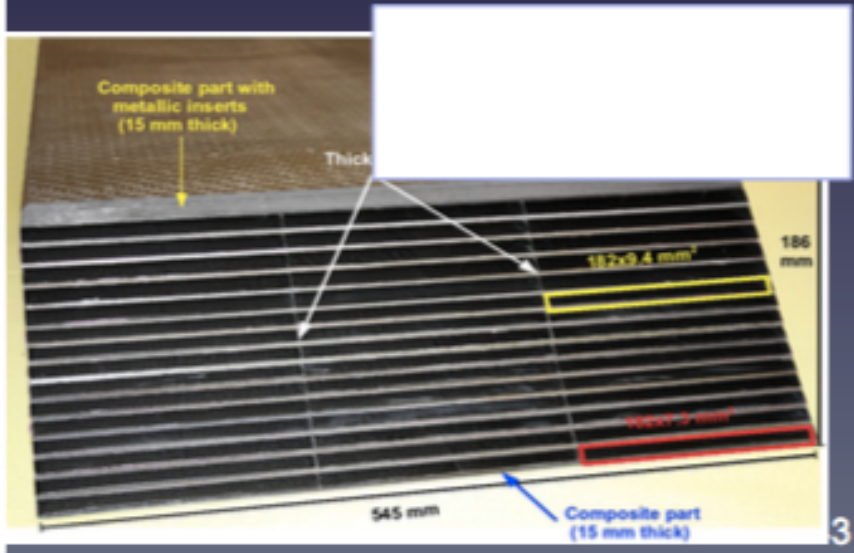
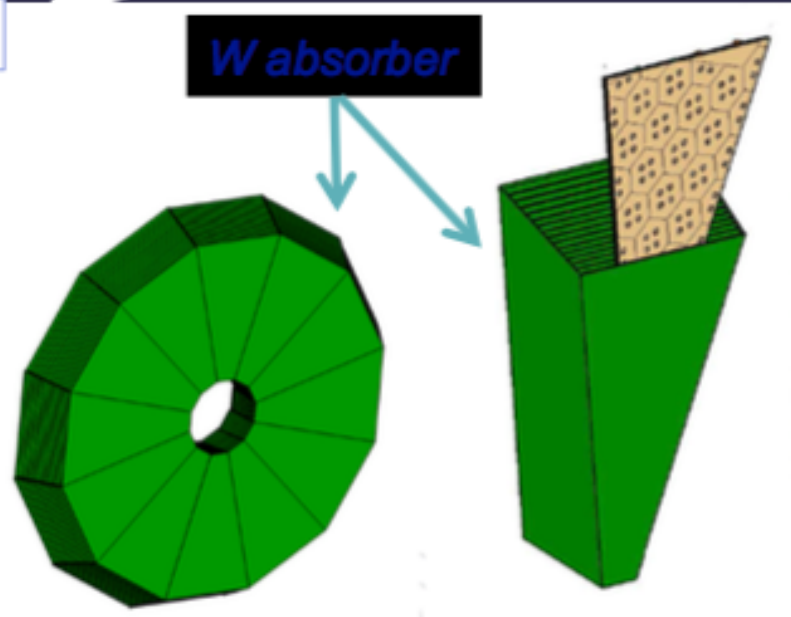
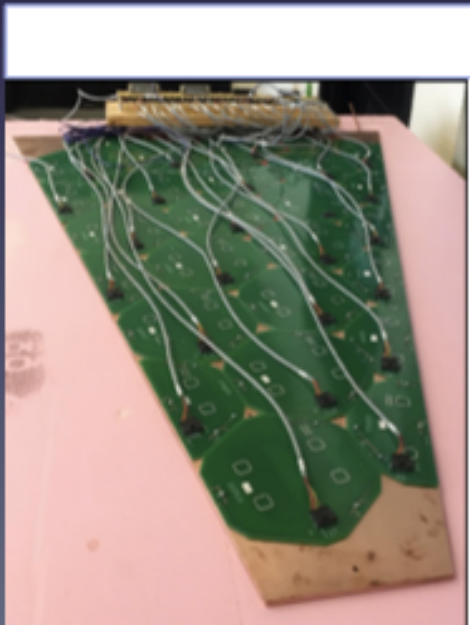
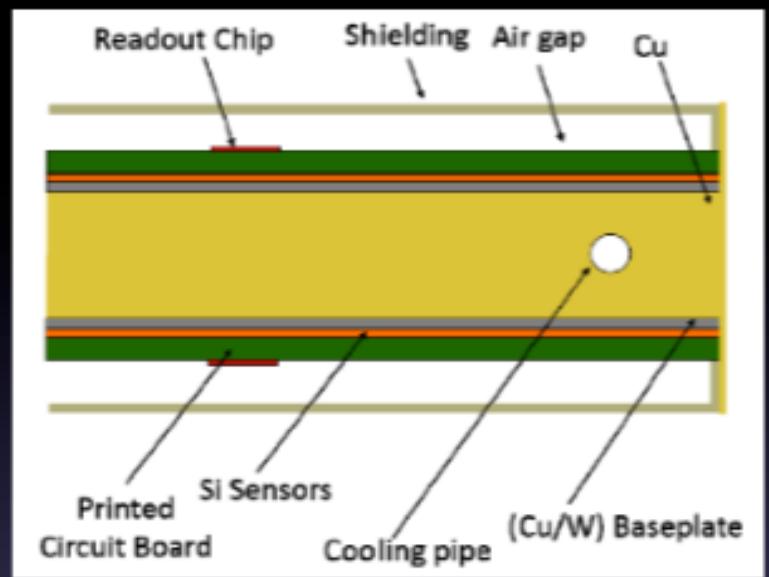
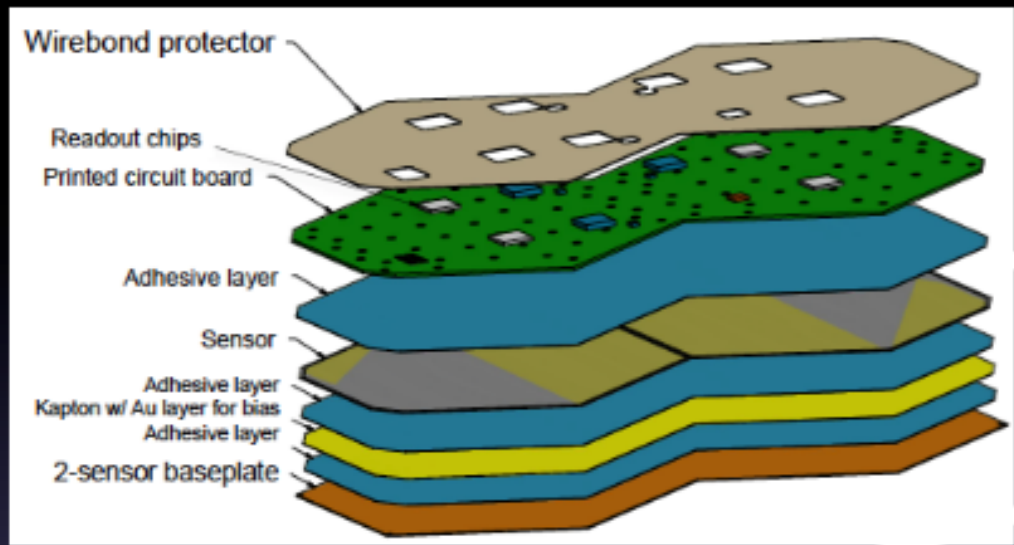
$12 \times 0.45\lambda$

Total Depth $> 10\lambda$

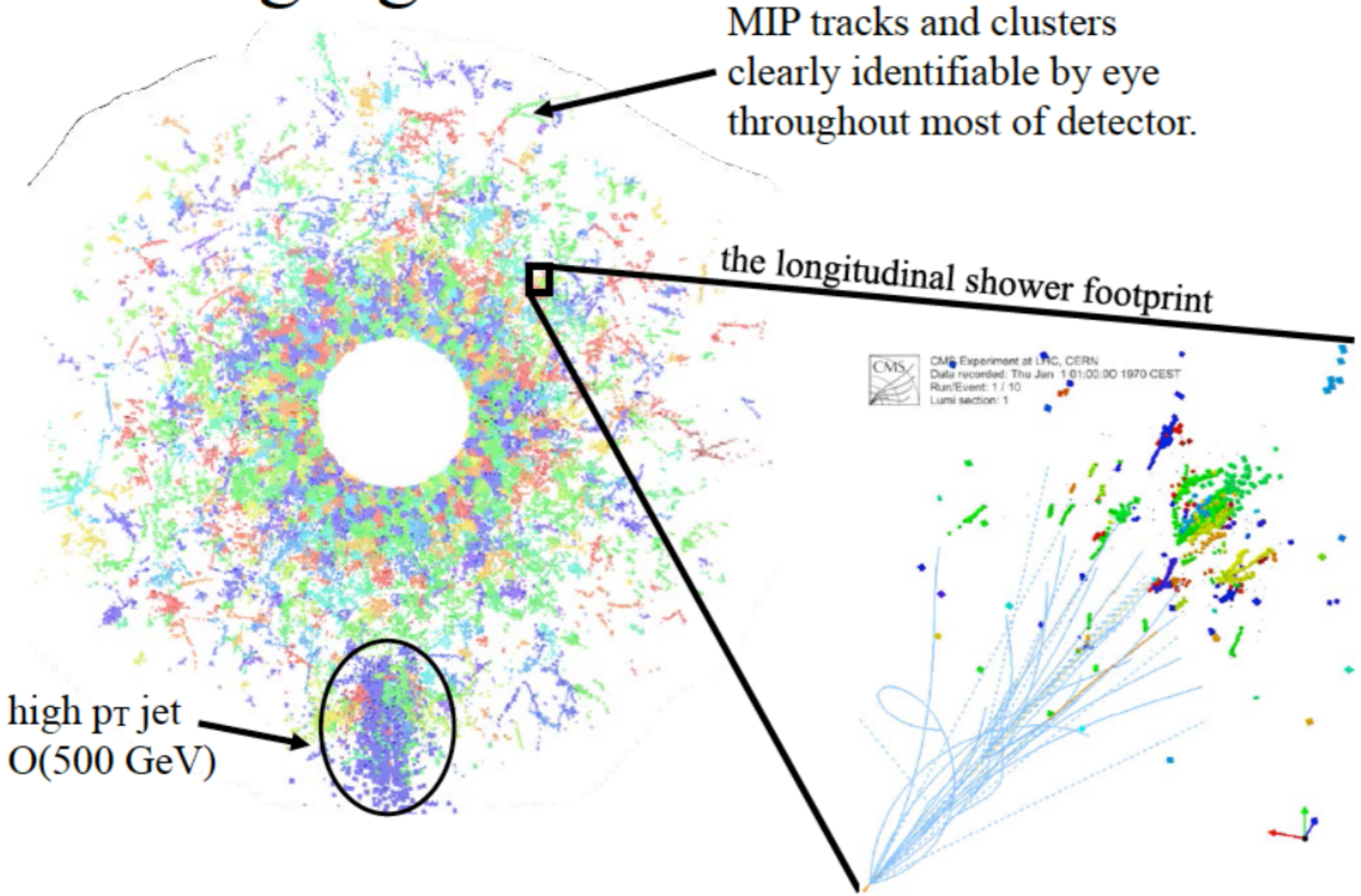
Table 3.2: Parameters of the EE and FH.

	EE	FH	Total
Area of silicon (m^2)	380	209	589
Channels	4.3M	1.8M	6.1M
Detector modules	13.9k	7.6k	21.5k
Weight (one endcap) (tonnes)	16.2	36.5	52.7
Number of Si planes	28	12	40

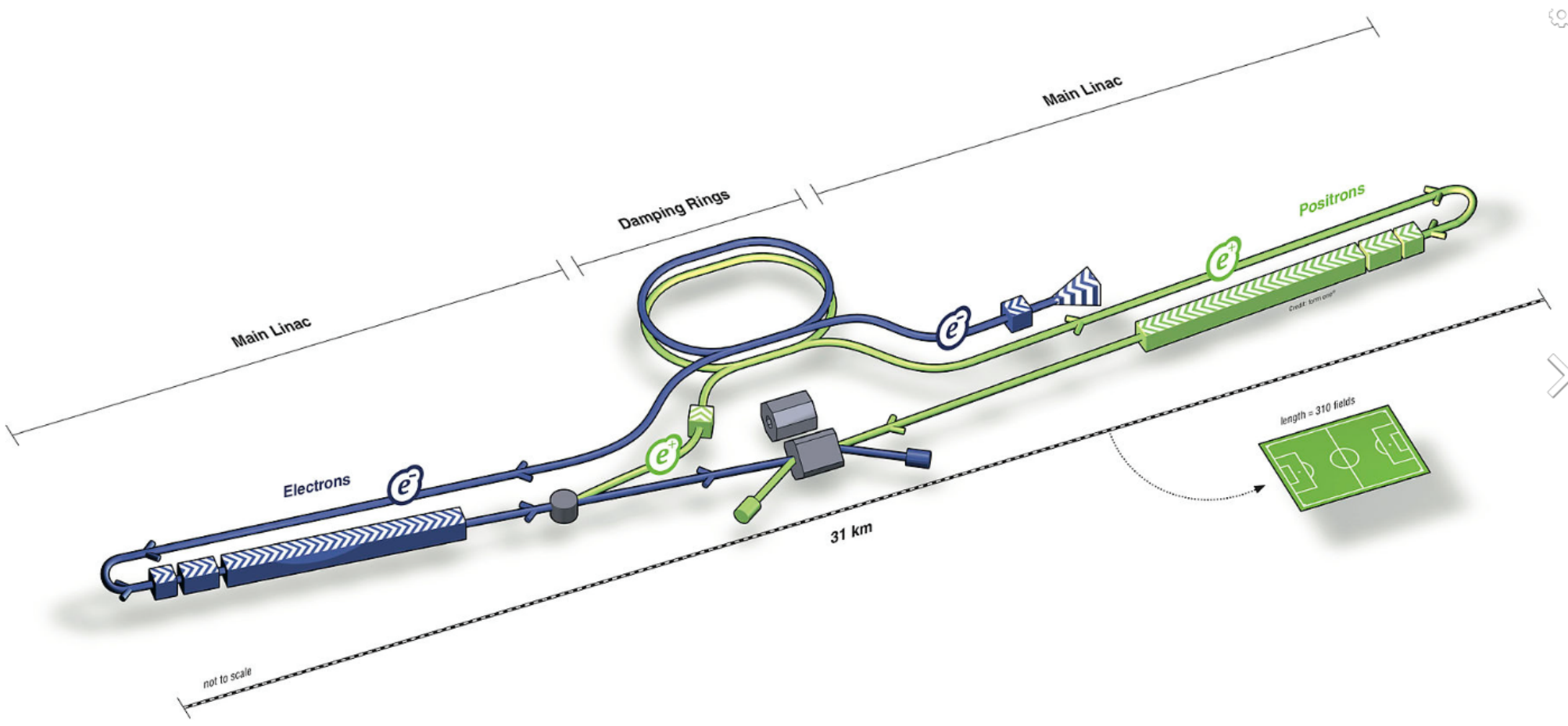
THINLYLY SEGMENTED ENDCAP ECAL FOR CMS



Imaging Showers with the HGC

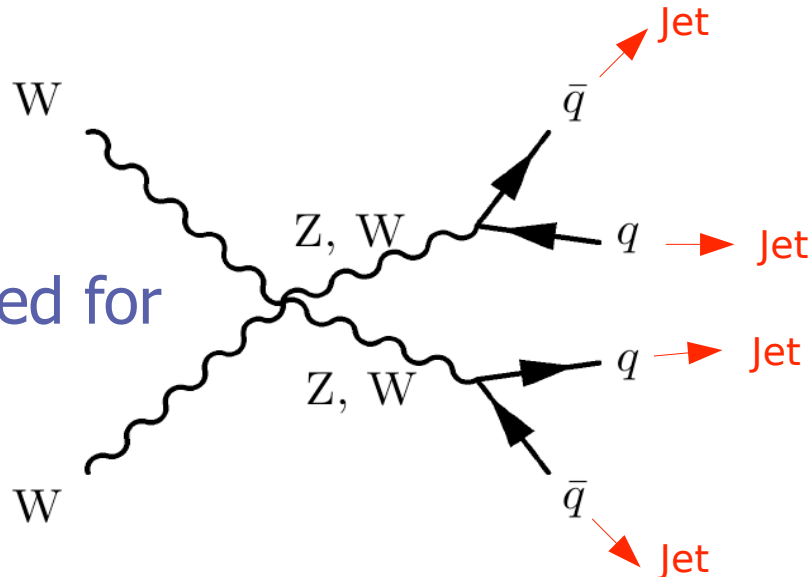


FUTURE LINEAR COLLIDER

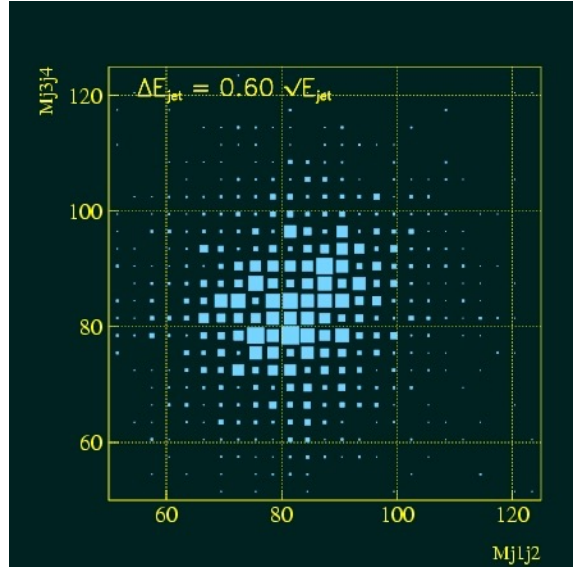


POSSIBLE FUTURE LINEAR COLLIDER (e-e)

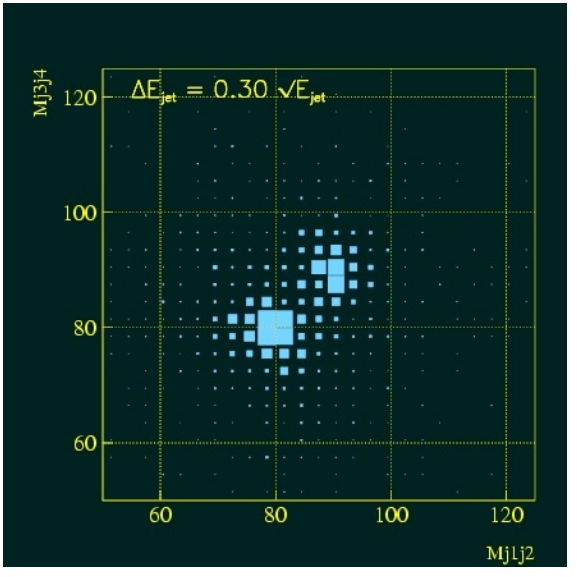
Boson-Boson scattering
 Hadronic Decay of W & Z
 Needs improved energy resolution
 Highly granular calorimeters optimized for particle flow



$\Delta(M_Z, M_W) \sim 10 \text{ GeV}$



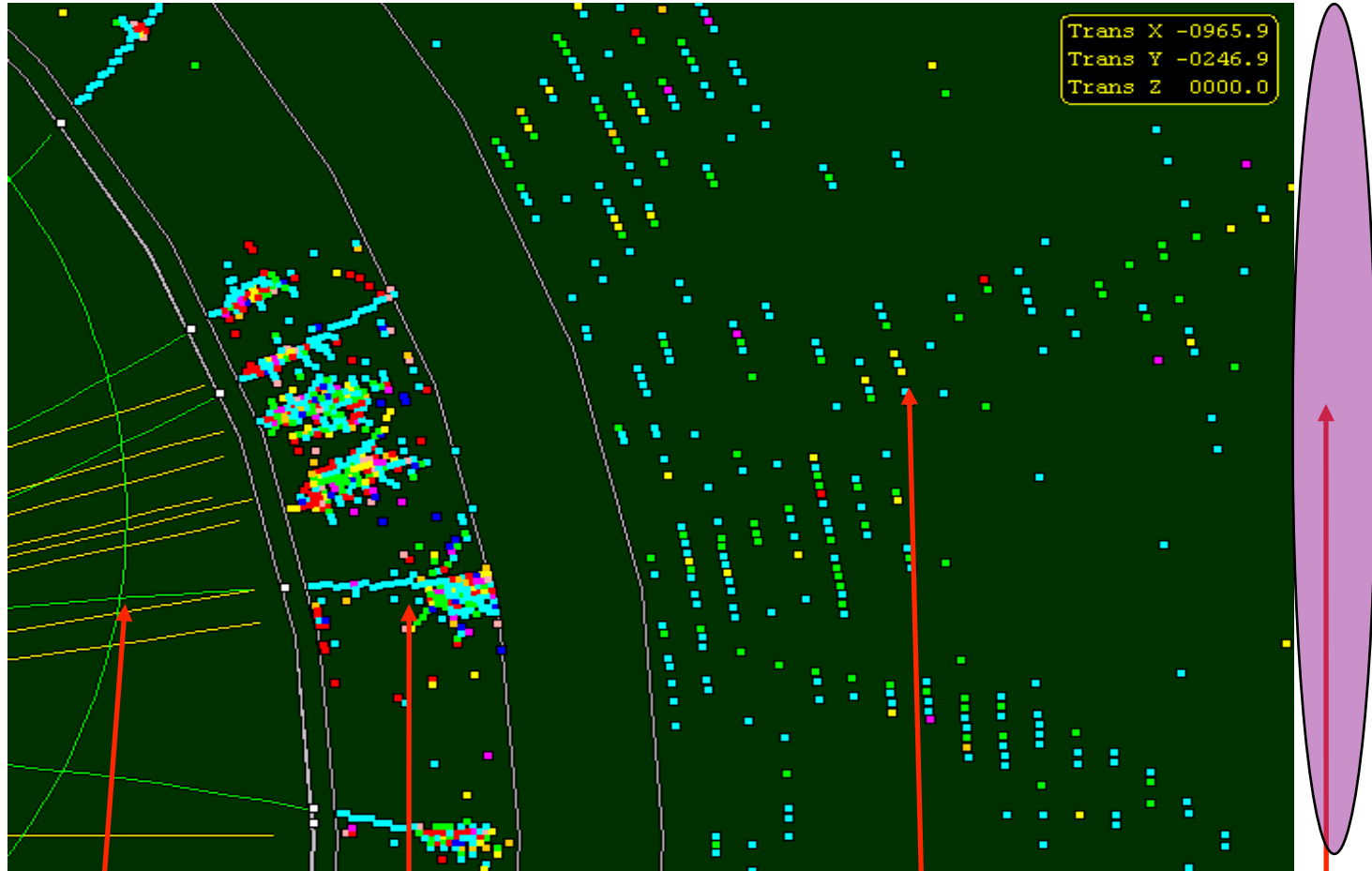
60%/√E



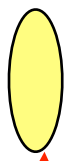
30%/√E



Highly segmented calorimeters



Trans X -0965.9
Trans Y -0246.9
Trans Z 0000.0



VXD
tag b,c
jets



Tracking
system



EM Cal



HAD Cal



Muon
system

FUTURE CIRCULAR COLLIDER ?

TO PROBE MATTER FURTHER.

Future Circular Collider

Circumference: **80-100 km**

Energy: **100 TeV (pp)**
>350 GeV (e^+e^-)

Large Hadron Collider

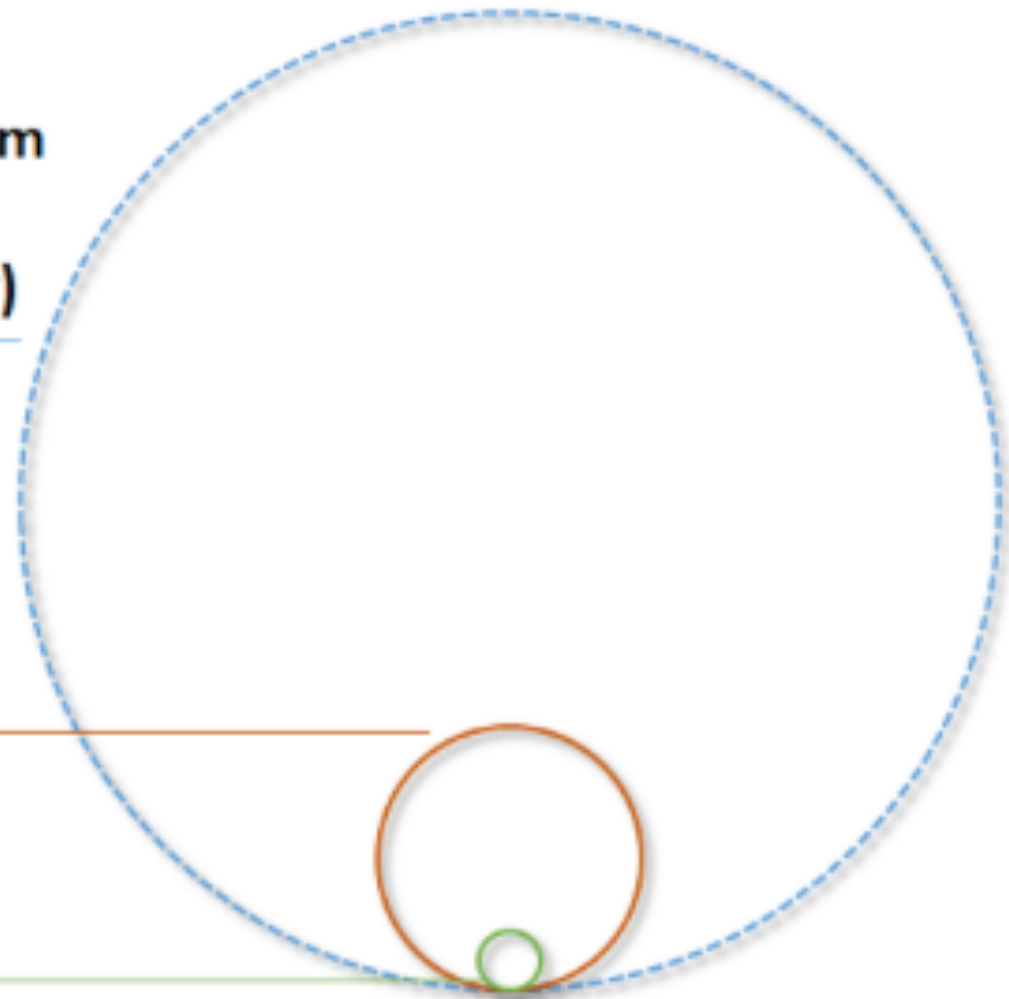
Circumference: **27 km**

Energy: **14 TeV (pp)**
209 GeV (e^+e^-)

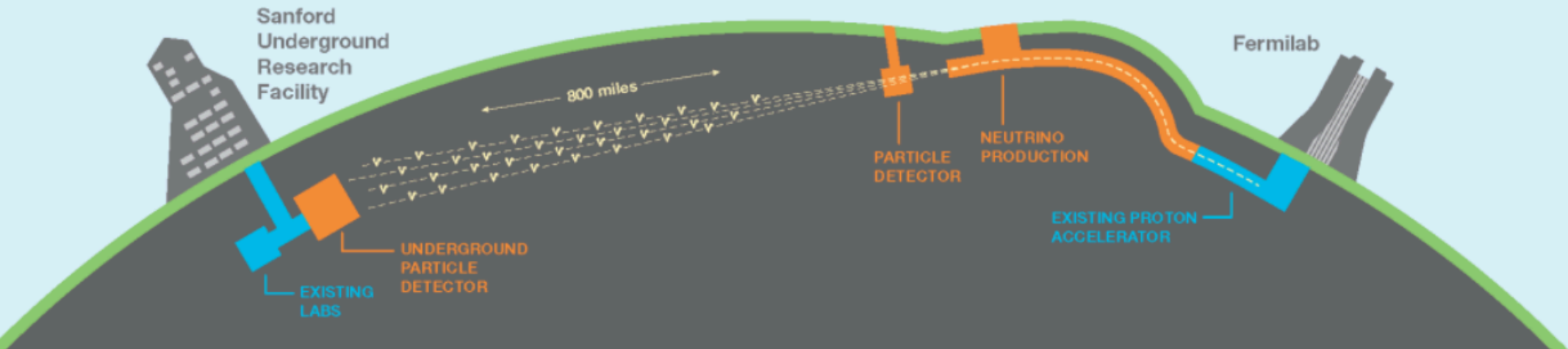
Tevatron (closed)

Circumference: **6.2 km**

Energy: **2 TeV**



THE DUNE PROJECT

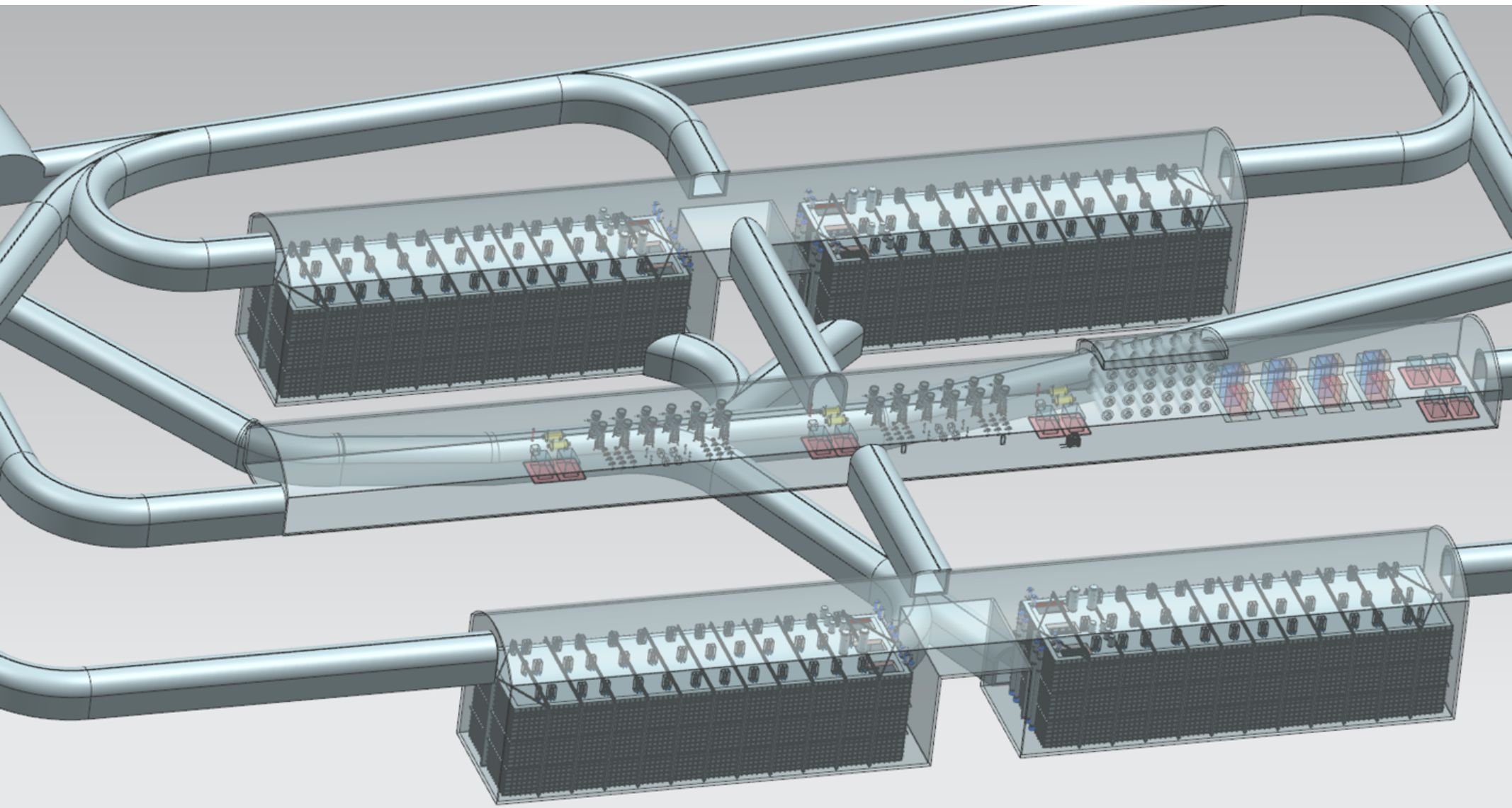


DUNE is an international project based in USA. It is a long base line experiment: neutrinos are produced at Fermilab (near Chicago), travel 800 miles underground before reaching a particle detector.

The aim of the experiment is to precisely measure the neutrino sector.

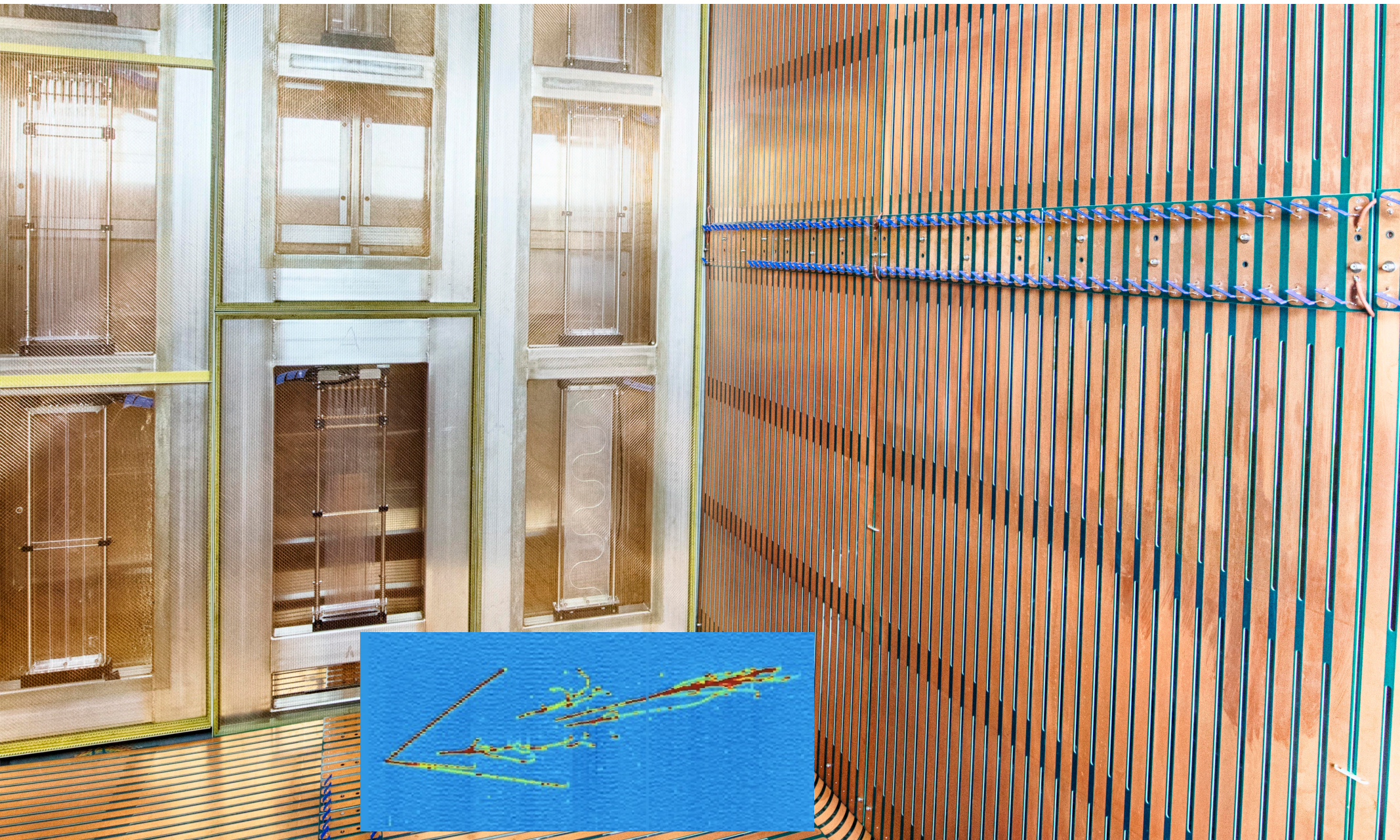
$$\begin{bmatrix} \nu_e \\ \nu_\mu \\ \nu_\tau \end{bmatrix} = \begin{bmatrix} U_{e1} & U_{e2} & U_{e3} \\ U_{\mu1} & U_{\mu2} & U_{\mu3} \\ U_{\tau1} & U_{\tau2} & U_{\tau3} \end{bmatrix} \begin{bmatrix} \nu_1 \\ \nu_2 \\ \nu_3 \end{bmatrix} \quad \begin{bmatrix} 0.82 \pm 0.01 & 0.54 \pm 0.02 & -0.15 \pm 0.03 \\ -0.35 \pm 0.06 & 0.70 \pm 0.06 & 0.62 \pm 0.06 \\ 0.44 \pm 0.06 & -0.45 \pm 0.06 & 0.77 \pm 0.06 \end{bmatrix}$$

THE DUNE PROJECT



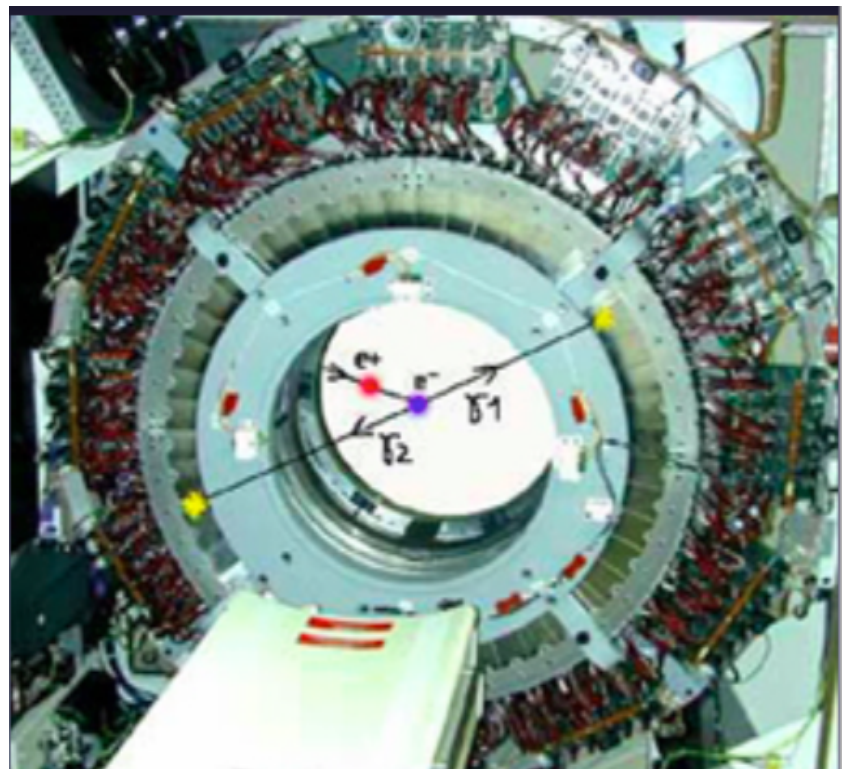
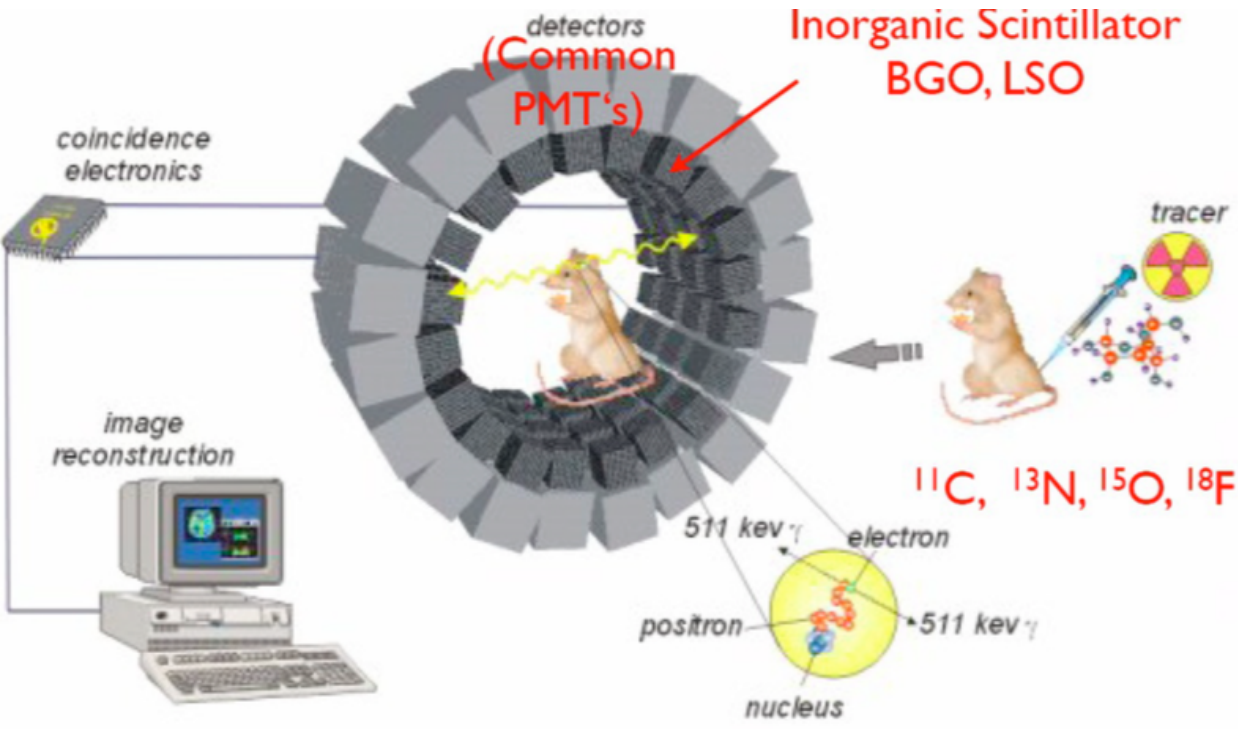
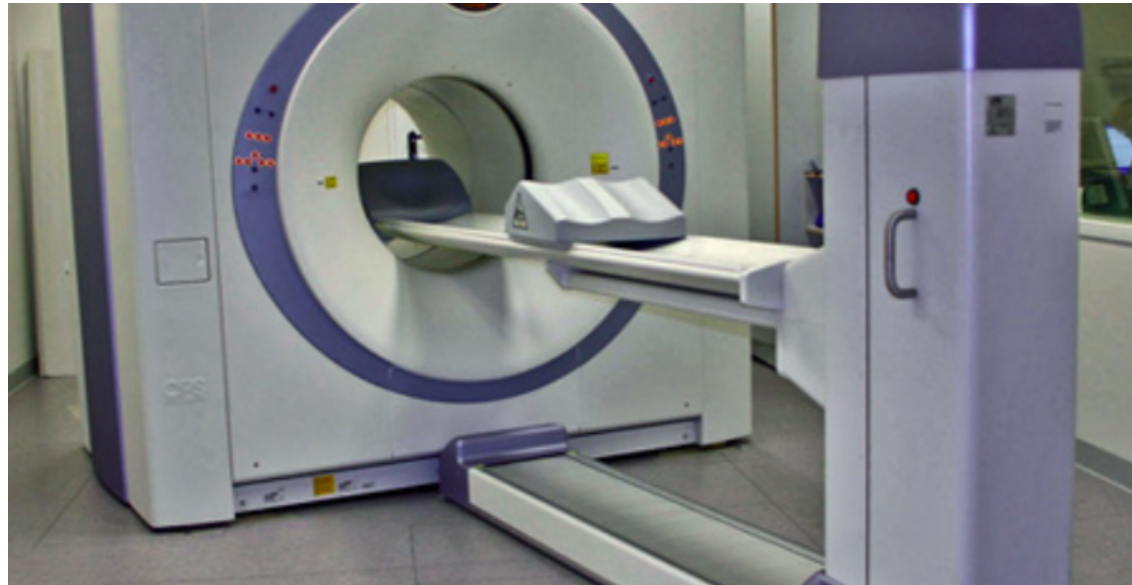
4 large liquid argon TPC - 17000 tons of argon

DUNE Liquid Argon Time Projection Chamber



APPLICATIONS of HEP TECHNIQUES: PET

Photo-Electron Tomography



SOME CONCLUSIONS

Detectors are designed and built to make specific physics measurements i.e. detectors are very specific for each physics subject

Detector techniques are based on particle interaction with matter ultimately on very low energy interactions.

The detector properties and their performance are the key to high quality physics results.

Instrumentation is evolving fast; physics requirements are increasing (rarer and rarer processes, precision measurements): each generation of detector has improved performance with respect to the preceding generation.